الجمهورية الجزائرية
الديمقراطية
الشعبية

People's Democratic Republic of Algeria

وزارة التعليم العالي والبحث
العلمي

Ministry of Higher Education and Scientific Research

جامعة العربي
التبسي – تبسة

University of Larbi Tébessi –Tebessa–

Faculty of Science and Technology

Department of Mechanical Engineering

Ref:

MASTER'S DISSERTATION

Mechanical Engineering

Option:

Materials Engineering

Presented by:

Fares Ziad

Effect of solution molarity on physical properties of Nickel oxide thin films prepared by spray pyrolysis method.

Jury:

Mr. KHELIFA Hocine	MCB	Tebessa University	President
Mr. DIHA Abdallah	MCA	Tebessa University	Supervisor
Mrs. BOULEDROUA Basma	MAA	Tebessa University	Examiner

University year: 2020 / 2021


بسم الله الرحمن الرحيم


ٱللَّهُ نُورُ ٱلسَّمَٰوَٰتِ وَٱلْأَرْضِ ۚ مَثَلُ نُورِهِۦ كَمِشْكَوٰةٍ فِيهَا مِصْبَاحٌ ۖ
ٱلْمِصْبَاحُ فِى زُجَاجَةٍ ۖ ٱلزُّجَاجَةُ كَأَنَّهَا كَوْكَبٌ دُرِّىٌّ يُوقَدُ مِن شَجَرَةٍ
مُّبَٰرَكَةٍ زَيْتُونَةٍ لَّا شَرْقِيَّةٍ وَلَا غَرْبِيَّةٍ يَكَادُ زَيْتُهَا يُضِىٓءُ وَلَوْ لَمْ
تَمْسَسْهُ نَارٌ ۚ نُّورٌ عَلَىٰ نُورٍ ۗ يَهْدِى ٱللَّهُ لِنُورِهِۦ مَن يَشَآءُ ۚ وَيَضْرِبُ
ٱللَّهُ ٱلْأَمْثَٰلَ لِلنَّاسِ ۗ وَٱللَّهُ بِكُلِّ شَىْءٍ عَلِيمٌ ٣٥

DEDICATION

First and foremost, I would like to thank ***ALLAH*** *for helping me to learn this quest of knowledge.*

I dedicate my dissertation work To …….

The lights of my life

FATHER & Mother

The lights of my eyes

My lovely Wife

Brother, Sisters and My Friends

My supervisor and teachers

All faithful hearts who helped me in the journey of my life.

TABLE OF CONTENTS

LIST OF FIGURES

CHAPTER 01 : BIBLIOGRAPHICAL STUDY

CHAPTER 2: METHODS OF DEPOSITION AND CHARACTERIZATION

CHAPTER 03: EXPERIMENT, RESULT AND DISCUSSION

LIST OF TABLES

LIST OF SYMBOLS

Symbol	Meaning	Unit
A	Absorbance	-
a ^{2}	Atomic distance	nm
$\mathbf{a_o}$	Lattice Constant	Å
$\mathbf{A_S}$	Area	Cm^2
C	The concentration	mol/l
$\mathbf{D_{av}}$	The Crystallite Size	nm
$\mathbf{d_{hkl}}$	Inter-planner Spacing	Å
$\mathbf{D_{hkl}}$	The average grain size	-
E	The chemical equivalent weight	g
$\mathbf{E_g}$	Energy Band gap	eV
$\mathbf{E_u}$	Urbach energy	meV
F	constant called the Faraday	-
hkl	the miller indices	-
hv	Photon Energy	eV
I	The current	A
$\mathbf{I_A}$	Absorbed light intensity	mW/cm^2
$\mathbf{I_o}$	Incident intensity	mW/cm^2
m	Mass Molar	g
M	Molar mass	mol
N	Reflection number	-
$\mathbf{N_0}$	The number of crystallites	cm^{-2}
P	The pressure	bar
$\mathbf{R_b}$	The bulk resistivity	Ω/Cm

$\mathbf{R_s}$	Sheet resistance	Ω/square
T	The time	s
t	The thickness	nm
T	Transmittance	-
$\mathbf{T_C}$	Texture Coefficient	-
V	The volume	L
W	The mass	g
A	The expansion coefficients	K^{-1}
$\boldsymbol{\beta_{hkl}}$	The full width at half maximum intensity	-
Δ	Dislocation Density	cm^{-2}
$\boldsymbol{\Delta_m}$	The weight difference	g
E	The strain	-
Θ	Diffraction Angle	Degree
Λ	Wavelength of Incident Light	nm
$\boldsymbol{\rho_0}$	The Density of Material	g/cm^3

LIST OF ABBREVIATIONS

Symbol	Meaning
ASTM	American Standard for Testing of Materials
CBD	Chemical Bath Deposition
CS	Cathode Sputtering
CVD	Chemical Vapor Deposition
EUV	Evaporation Under Vacuum
F.C.C	Face-Centered Cubic
JCPDS	Joint Committee for Powder Diffraction Standards
Ni	Nickel
NiO	Nickel Oxide
PLD	Pulsed Laser Deposition
SPT	Spray Pyrolysis Technique
TBL	Thermal Barrier Layer
TCO	Transparent Conductive Oxides
TE	Thermal Evaporation
UVS	UV-visible Spectrophotometer
XRD	X-Rays Diffraction

Materials sciences and Engineering

GENERAL INTRODUCTION

GENERAL INTRODUCTION:

In recent years nanotechnology has developed into one of the most prominent and exciting forefront fields in Physics, chemistry, engineering and biology. Nanoparticles and nanostructures fabricated with the use of nanotechnology present new properties and characteristics that can be utilized in a wide variety of applications. Its impacts a broad range of fields such as material engineering, medicine, energy, environment, defense, security and electronics [1].

According to this context, it was a main motive for this research to enter the experimental world of nanotechnology, to see the microscopic changes that occur in the material and how we can exploit them scientifically in different applications.

Nickel oxide is the chemical compound with the formula NiO and it is the only well characterized oxide of nickel. The mineralogical form of NiO, bunsenite, is very rare. NiO can be prepared by multiple methods.

Upon heating above 400 °C, nickel powder reacts with oxygen to give NiO. In some commercial processes, green nickel oxide is made by heating a mixture of nickel powder and water at 1000 °C, the rate for this reaction can be increased by the addition of NiO [Pradniak 2002].The simplest and most successful method of preparation is through pyrolysis of a nickel compounds such as the hydroxide, nitrate, and carbonate, which yields a light green powder. Synthesis from the elements by heating the metal in oxygen can yield grey to black powders which indicates nonstoichiometric [Greenwood and Earnshaw 1984].NiO adopts the NaCl structure, with octahedral Ni and O_2 .Nickel oxide (NiO) has a density of (6.67 g/cm), molecular weight of (74.69 g/mol) and its melting point is (1955^{o}C) [11-12].

Nickel oxide thin films have different applications such as, an antiferromagnetic material type transparent conducting films [Sato et al.1993], electro catalysis, positive electrode in batteries, fuel cell, a material for electro-chromic display devices, solar thermal absorbers, etc [13].

Different techniques such as sol–gel, spray pyrolysis, ion beam sputtering, magnetic sputtering, and pulsed laser deposition have been used for deposition of NiO films [47].

In the present research, we report the effect of solution molarity on the electrical and optical properties of NiO thin films prepared by chemical spray pyrolysis technique.

This study aims to achieve two main objectives:

- Installation of a homemade device, allows the preparation of thin films of metal oxides, by method of chemical spray pyrolysis.
- Preparation of Nano structuring thin films of Nickel oxide, and study their optical and electrical properties.

This work consists of three chapters organized, starting with a general introduction.

The first chapter is bibliographical study which describing Thin films and give a general view of metal oxide properties and their application focusing on Nickel oxide.

The second chapter will explain some preparation methods of thin films and we will focus on the method of spraying pyrolysis, then we will describe the various characterization techniques to analyze thin films.

The third chapter explains the several steps of experiment and shows the homemade devices used in preparation of Nano structuring thin films of Nickel oxide and give the optical and electrical characterization results.

Finally, there will be a conclusion present the synthesis of main results obtained, concluding remark.

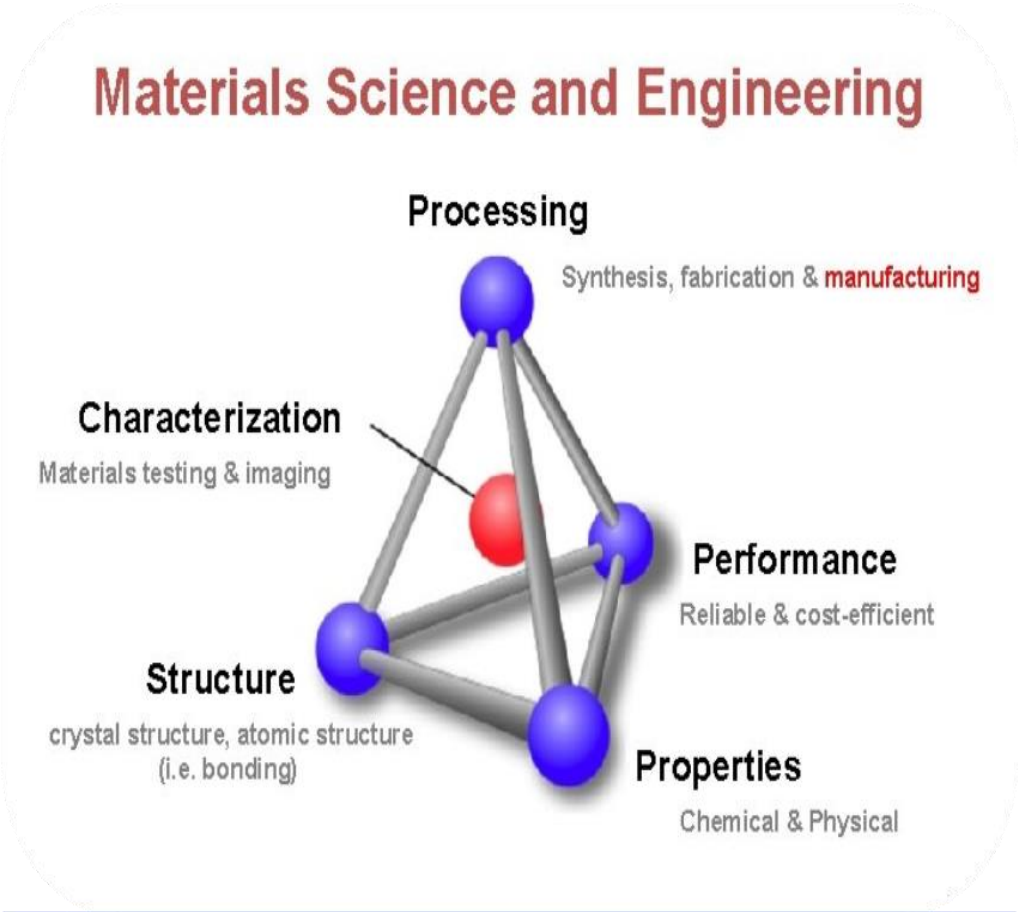

CHAPTER 1 : BIBIIOGRAPHICAL STUDY

I.1. Introduction:

This first chapter gives a bibliographic overview of thin films by giving their definition, application and also the principal of deposit and the growth mechanism. Nickel oxide (NiO) by introducing their structural, optical and electrical properties. We will also present a general outline of the potential applications of metal oxides including solar cells, photodetectors and the photocatalysis application.

I.2. Definition of thin films:

A thin film of a material can be define that is an element of this material so that its thickness is greatly reduced, which is expressed with nanometers (1 to 100 m^{-9}).The small distance between the two boundary surfaces gives a disturbance of the physical, chemical and mechanical properties (fig 1.1). The essential difference between the material it's in the bulk state and it's the thin state related to the fact that the role of the boundaries in the properties is usually neglected in the bulk state of materials, but in the thin state, on the contrary, the effects related to the boundaries are preponderant and very important [1]. It is quite obvious that the lower the thickness, the greater the bidimensionality effect. Conversely, when the thickness of a thin layer exceeds a certain threshold, the effect of thickness will become minimal and the material will return to the well-known properties of the solid state of material [2]. The second essential characteristic of a thin layer is that, whatever the procedure used for its manufacture, a thin layer is always integral with a substrate on which it is built (even if it sometimes happens that one separates the thin film of said substrate). Consequently, it will be imperative to take into account this major fact in the design, namely that the substrate has a very strong influence on the structural properties of the layer deposited therein. Thus a thin layer of the same material, of the same thickness may have substantially different physical properties depending on whether it will be deposited on an amorphous insulating substrate such as glass, or a monocrystalline silicon substrate, for example. The purpose of the thin layer is to give particular properties to the surface of the part while benefiting from the massive properties of the substrate (in general: mechanical resistance), for example:

* Electrical conductivity: metallization of the surface, for example to observe an insulating sample under a scanning electron microscope.

* Optical: mirror glass, anti-reflective treatment of camera lenses, nickel plating of fire helmets to reflect heat (infrared), gilding of their visor to avoid glare.

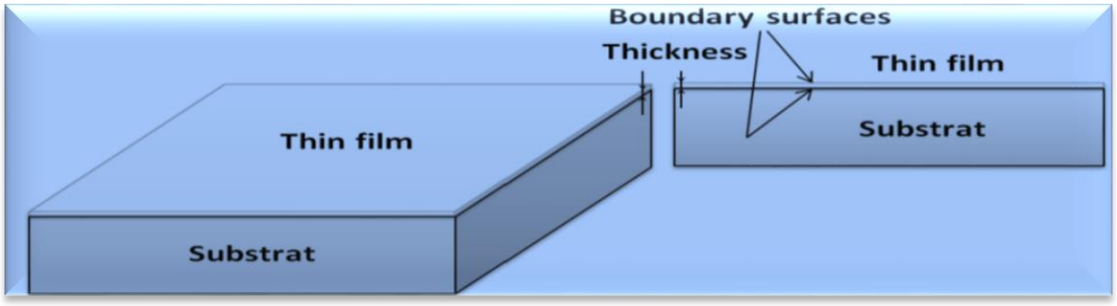

Figure 1.1: Schematic of thin film deposited on a glass substrate [2].

I.3. Principle of deposit of thin films:

To form a thin layer on a solid surface (substrate) the particles of the coating material must pass through a conductive medium until intimate contact with the substrate. When the substrate arrives, a fraction of the coating particle adheres or reacts chemically with the substrate. The particles can be atoms, molecules, ions or fragments of ionized molecules. The transport medium can be solid, liquid, gas, or vacuum:

a) Solid: in this situation, the substrate is in contact with the solid, only the particles which diffuse from the solid towards the substrate form a layer. Often, it is very difficult to obtain thin films by contact between solids, for example: the diffusion of Oxygen from Silica to form a thin SiO2 layer on a Silicon substrate.

b) Liquid medium: it is easier to use than the first case, because the material is more versatile in this state (epitaxy in liquid phase, and electrochemical, sol gel…).

c) Gas or vacuum: this is a CVD type deposit where the difference between the gaseous medium and the vacuum is the average free path of the particles. There is no standard thin film deposition method that can be used in different situations. Substrate preparation is often a very important step for thin layer deposits in order to obtain good adhesion [3].

I.4. Formation of thin films:

The process of depositing a thin layer is carried out in three stages [4]:

- Synthesis or creation of the species to be deposited.
- Transport of these species from the source to the substrate.

- Deposition on the substrate and growth of the layer.

Depending on the process followed, these steps can be completely separate from each other or else superimposed. Figure I.2 illustrates, in general, the process steps involved in the development of thin layers [5].

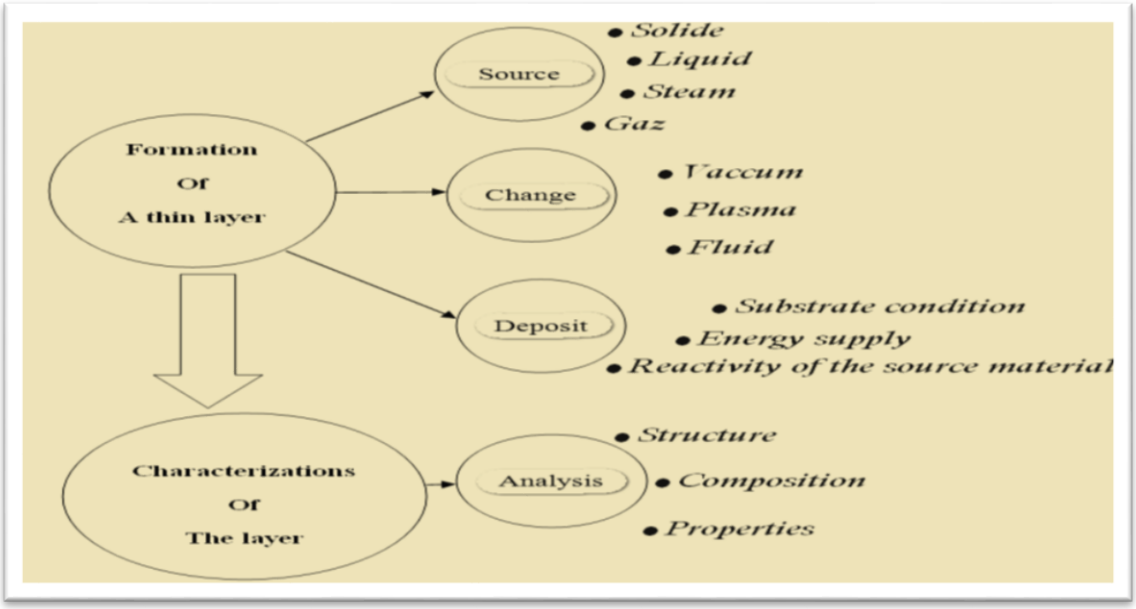

Figure I.2: Diagram of the steps of the thin film manufacturing process [5]

I.5. Interest and characteristics of thin film:

The interest of thin film is to give particular properties to the surface of the substrate

The major interest of thin layers is the economical use of materials in relation to the physical properties and the simplicity of the technologies used for their realization. The essential difference between the material in the its bulk state and its the thin state is related to the fact that the role of the boundaries in the properties is usually neglected in the bulk state of materials, but in the thin state, on the contrary, the effects related to the boundaries are preponderant and very important. It is quite obvious that the lower the thickness, the greater the bidimensionality effect. Conversely, when the thickness of a thin layer exceeds a certain threshold, the effect of thickness will become minimal and the material will return to the well-known properties of the solid state of material. The second essential characteristic of a thin layer is that, whatever the procedure used for its manufacture, a thin layer is always integral with a substrate on which it is built (even if it sometimes happens that one separates the thin film of said substrate). Consequently, it will be imperative to take into account this major fact in the design, namely that the substrate has a very strong

influence on the structural properties of the layer deposited therein. Thus a thin layer of the same material, of the same thickness may have substantially different physical properties depending on whether it will be deposited on an amorphous insulating substrate such as glass, or a monocrystalline silicon substrate, for example [6] .

I.6. Thin film growth mechanism:

All thin film processes are done in three stages:

- The production of appropriate ionic, molecular, atomic species.
- The transport of these species to the substrate.
- Condensation on this same substrate is done either directly or through a chemical or electrochemical reaction in order to form the solid deposit; this step often goes through three phases: nucleation, coalescence then growth.

a) Nucleation

It is the phenomenon that accompanies changes in the state of matter and which consists in the appearance, within a given medium, of transformation points from which a new physical or chemical structure develops.

The entire surface of it, in this state, they interact with each other and form what are called "clusters". These "clusters" also called nuclei, are unstable and tend to subside. Under certain deposit conditions, they collide with other adsorbed species and start to grow. After reaching a critical size, these clusters become thermodynamically stable and the nucleation barrier is crossed. The nucleation stage is shown in figure I.3.

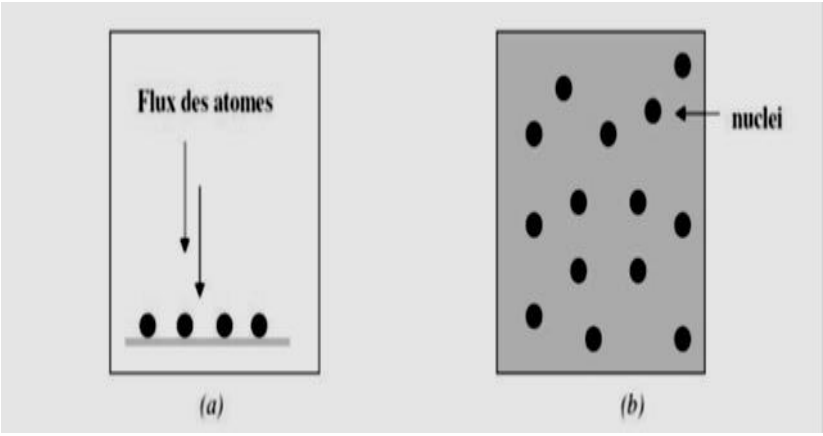

Figure I.3: Diagram of the nucleation of thin layers. a) The arrival of atoms on a substrate, b) The morphology of the substrate [7].

b) Coalescence

The nuclei grow in size but also in number until they reach a maximum nucleation density. This as well as the average size of these nucleus also called islets depend on a certain number of parameters such as the energy of the sprayed species, the rate of spraying, the energy of activation, adsorption, desorption, thermal diffusion, substrate temperature, topography and chemical nature of the substrates .

A nucleus can grow at the same time parallel to the substrate by a surface diffusion phenomenon of the pulverized species. It can also grow perpendicular to the substrate by adding sprayed species. In general the lateral growth in this stage is much more important than the perpendicular growth. figure I.4 represents the phase of coalescence.

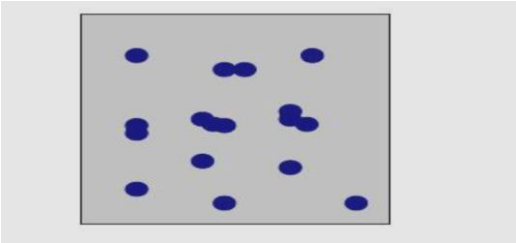

Figure I.4: Diagram representing coalescence [7].

c) Growth:

The last step in the film manufacturing process is the coalescing step in which the islets begin to cluster. This tendency to form larger islets is improved by the growth of the surface mobility of the adsorbed species. This improvement is obtained by increasing the temperature of the substrate. These larger islets still grow, leaving channels and holes on the substrate. The structure of the film in this step changes from a type of discontinuous islands to a type of porous networks .A continuous film is formed by filling the channels and the holes [7].

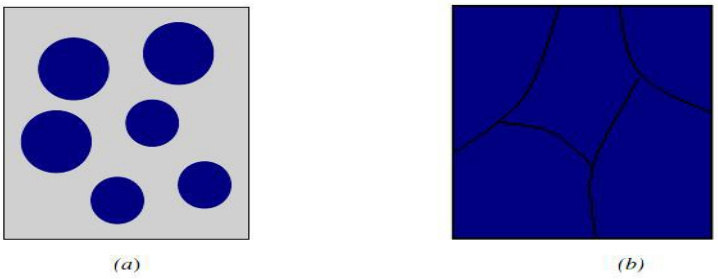

Figure I.5: The growth of thin layers. a) Step after coalescence, b) Growth [7].

I.7. Applications of thin films:

During 20th century, more sophisticated applications diversified in the following fields [8-9].

- **Microelectronics:** It was developed from the 1960s thanks to the use of increasingly thin conductive or insulating layers, and can be found under types of passivating layers (electronic contact), PN junction, transistor diode, piezoelectricity, laser, LED lamps, superconductors, etc.
- **Optics:** While retaining the aesthetic applications, the optical applications of the layers have made it possible to develop more effective radiation sensors, such as antireflective layers in solar cells, anti-reflective treatment of camera lenses, photo detection, display of screens dishes, ophthalmic applications, optical guides (architecture energy checks, vehicles, energy conversion, etc.).
- **Mechanics:** Tribological coatings (dry lubrication, resistance to wear, erosion, abrasion, diffusion barriers) micro-systems…etc.
- **Chemistry:** The main applications of surface coatings are oriented towards better corrosion resistance by the creation of a waterproof film (corrosion resistance), gas sensor, catalytic coatings and protective layers.
- **Thermal:** The use of a thermal barrier layer (TBC) decreases for example the surface temperature of the metal of the fins of the reactors thus making it possible to improve the performances of the reactors (increase in the internal temperature).
- **Biology:** Biological micro sensors, biochips, biocompatible materials…etc.
- **Micro and Nanotechnologies:** Mechanical and chemical sensors, micro fluidics, actuators, detectors, adaptive optics, nano-photonics…etc.
- **Magnetic:** Information storage (computer memory), security devices, sensors.
- **Decoration:** Watches, glasses, jewelry, household equipment, etc [10].

I.8. General Properties NiO:

Nickel oxide is the chemical compound with the formula NiO. It is notable as being the only well characterized oxide of nickel. The mineralogical form of NiO, bunsenite, is very rare. NiO can be prepared by multiple methods. Upon heating above 400^{o} C, nickel powder reacts with oxygen to give NiO. In some commercial

processes, green nickel oxide is made by heating a mixture of nickel powder and water at 1000° C, in follow the general properties [11-12]:

- Average atomic number : 18
- Average atomic mass (g) : 27.35
- Molar mass (g / mol) : 74.69
- Boiling point (° C) > 2000
- Solubility in water (mg / L) : 1.1 at 20 ° C. insoluble
- Melting point (° C) : 1990 - 1960
- Enthalpy of formation at : 298k -240 KJ / mole of atoms
- Entropy S0 (KJ.mol-1) : 38.0

I.8.1. Crystallographic properties:

The nickel oxide (NiO) crystallizes in a cubic NaCl-type structure (rocksalt) as shown in fig I.6 and fig I.7**,** each cubic unit cell has four Nickel atoms and four Oxygen atoms. Each Nickel atom is bounded by six Oxygen atoms and the same thing for Oxygen atom has six Nickel atoms surrounding it. This face-centered cubic (F.C.C) structure has a parameter of 4.1769Å at 26°C. Along any one of its triad axes, the (F.C.C) structure has a primitive rhombohedral cell with α = 60°. Fig I.8 shows a rhombohedral unit cell in the face-centered cubic cell. For nickel oxide, X-ray diffraction shows that the cubic lattice is slightly shifted to give a structure of rhombohedral cell with α =60°4.2' at room temperature. The Nickel-Nickel distance is 2.9518A for the distorted rhombohedral (α =60°4.2' at 18°C), while this distance should be 2.9535Å for a cubic cell (α =60°and a= 4.1769Å). This departure from the ideal-face centered cubic structure also was found to be temperature dependent. The amount of the distortion increases with the decrease of temperature [13-14].

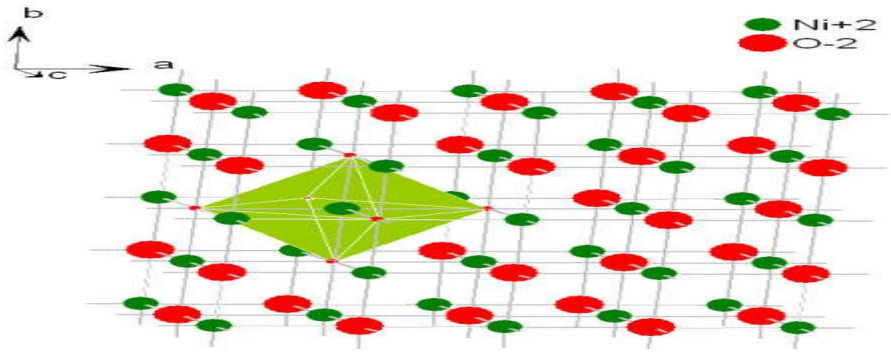

Figure I.6: The crystalline structure of NiO [11].

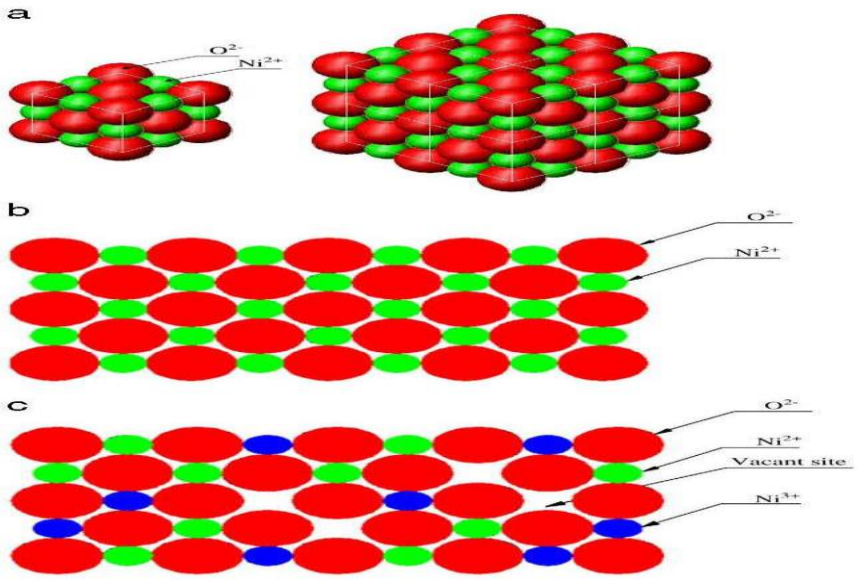

Figure I.7: Structure of nickel oxide.

a. Structure of nickel oxide in 3D

b. Structure of nickel oxide in 2D (Stoichiometric).

c. Structure of nickel oxide in 2D (Non-stoichiometric)[12].

I.8.2. Electrical properties of NiO:

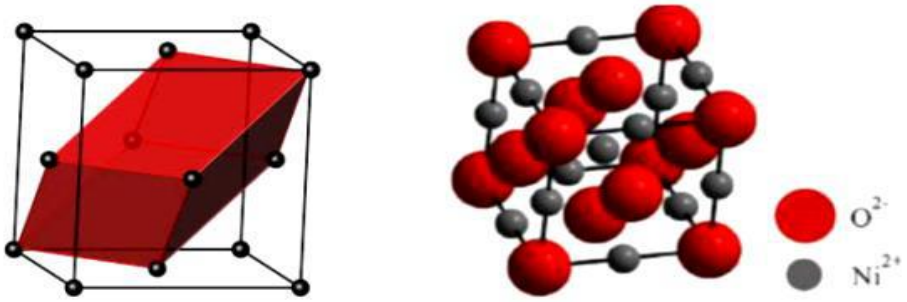

Figure I.8: The rhombohedral primitive cell of a face central cubic cell of Nickel Oxide [14].

Nickel oxide is a promising candidate for transparent conductive oxide with p-type conductivity. Stoichiometric undoped NiO is an insulator having a resistivity of 1013 Ω cm at room temperature [15].

Substantial conductivity can be achieved in NiO by creating Ni vacancies, forming interstitial oxygen atoms or doping with other cations mainly with monovalent Li ions [16-17].

The electrical properties of NiO films are related to their microstructure and their composition, and the annealing atmosphere. Jlassi M. *et al.* [17] reported that the

resistivity is about 900 × 103 Ω cm for the treated samples in air and about 40 Ω cm for the samples treated under nitrogen. Table I.1, gave some electrical properties of NiO.

For the nickel oxide the electronic configurations of the oxygen and nickel atoms are as follows:

O: $1s^2 2s^2 2p^4$,

Ni: $1s^2 2s^2 2p^6 3s^2 3p^6 3d^8 4s^2$

The NiO has been under extensive investigation for decades due to its interesting electronic structure, strongly affected by Ni 3d electrons that are localized in space, but spread over a wide range of energy due to strong Coulomb repulsion between them [19-20].

Table I.1 some electrical properties of NiO [21-22].

Properties	Values
Conductivity type	P
Electrical conductivity ($(\Omega.cm)^{-1}$)	10^{-6}_10^{-1}
Hall coefficient (cm^3/C)	5_120
charge carrier density (cm^{-3})	10^{17}_10^{18}
Mobility (cm^2/ V.s)	0.1_7.6

I.8.3. Optical properties of NiO:

Nickel Oxide is a bread band-gap semiconductor. The absorption edge is localized in the ultraviolet region, the existence of Ni^{+3}ions inner the oxide lattice shows charge transfer transition with the resulting absorption in the visible region [22-23].Various researchers have estimated the absorption of photon energy for NiO [24-25].Reported gap energy value for the NiO is in the range of 3.6 to 4 eV, however, the refractive index is 2.33 at the photon energy of 2 eV [26]. The valence band consists of localized Nickel 3d-bands with a width of 4.3-4.4eV [27-28] .at about 2eV above the Fermi level at –8.74 eV. Oxygen at the 2p band with large energy about 4–8 eV; were coupled with the Nickel 3d states. However, the conduction band composes of unoccupied states of Nickel 3d, 4s, and 4p [29]. Two main theories proposed for explaining the optical absorption gap in NiO: it is due to either a p→d transition in one Ni atom [30].or a d→ d transition throughout two adjacent Ni atoms in the lattice [31].

I.9. Applications of metal oxides:

Metal oxides play a very important role in many areas of chemistry, physics and materials science. The metal elements are able to form a large diversity of oxide compounds. These can adopt a vast number of structural geometries with an electronic structure that can exhibit metallic, semiconductor or insulator character. In technological applications, oxides are used in the fabrication of microelectronic circuits, sensors, piezoelectric devices, fuel cells, coatings for the passivation of surfaces against corrosion, and as catalysts. In the emerging field of nanotechnology, a goal is to make nanostructures or Nano arrays with special properties with respect to those of bulk or single particle species. Oxide nanoparticles can exhibit unique physical and chemical properties due to their limited size and a high density of corner or edge surface sites. Particle size is expected to influence three important groups of basic properties in any material.

I.9.1. Solar cells and photodetectors:

In general metal oxides (MO) are mostly non-toxic with obvious chemical stabilization and important abundance in nature, also manufactured using inexpensive methods under ambient conditions. MO-based devices are inexpensive, very stable, and environmentally safe. 10 years ago, it was difficult to use these materials as semiconductors but nowadays a lot of companies sell products based on these materials [33]. Thus, MO-based semiconductors are promising for third generation solar cells.

I.9.1.1 Solar cells:

Photovoltaic cells essentially work by utilizing the photovoltaic effect which defines by the ability of a p-n junction device to convert the incident sunlight into electricity. The p-n junction formatted when a p-type semiconductor material is brought into contact with an n type semiconductor material [34].

Figure I.9 illustrates the operating principle of a conventional photovoltaic cell called the first generation.

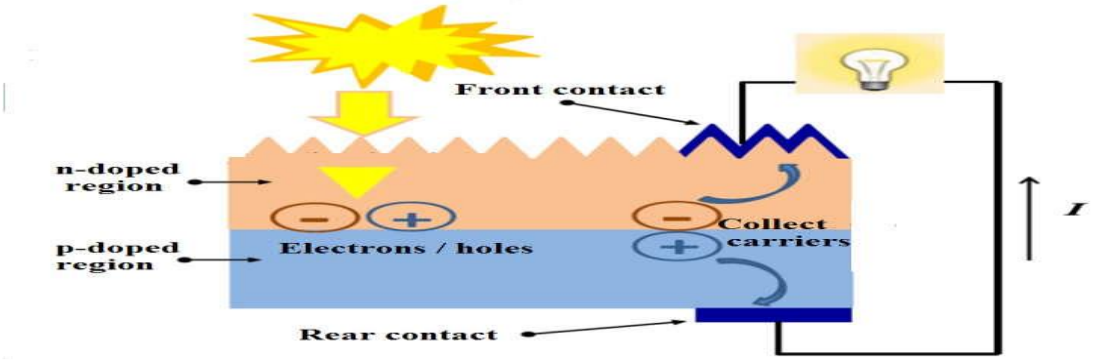

Figure I.9: Operation principle of a photovoltaic cell (first generation) [35].

When photons of incident light with energies greater than or equal to the band gap of the semiconductor material are absorbed by the p-n junction, electron/hole pairs are created. Electrons are excited from the valence band into the conduction band leaving holes at valence band and by collecting those charges the electric energy will produce.

I.9.1.2 Photodetectors:

Photodetectors are used in a variety of applications in many fields like compact disc players, optical-fiber communications, and surveillance of rockets or intercontinental ballistic missiles, remote sensing…. They are basically semiconductor devices that can detect an optical signal and convert it into an electrical signal. The operation of a general photodetector basically operates as a solar cell. Figure I.10 summarized the operating mechanism on three processes: first, carrier generation by incident light then second, carrier transport and/or multiplication then third, extraction of carriers as terminal current to provide the output signal [36]. Three main types of photodetectors are generally used: photoconductors, photodiodes, and phototransistors.

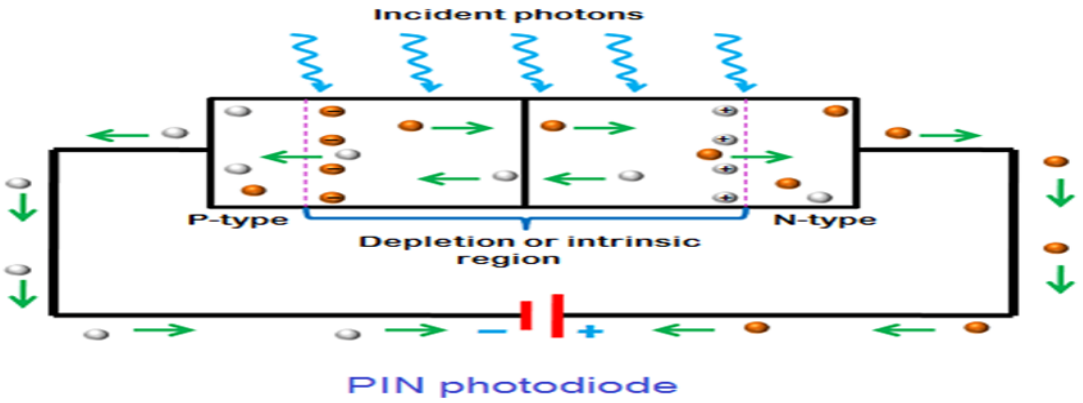

Figure I.10: Operating Mechanism of the photodiode p-n junction [36].

I.9.1.3 The basic principle of photocatalysis:

In the photocatalytic oxidation process, the organic pollutants are destroyed by the semiconductor photocatalyst (e.g., TiO2, ZnO, NiO) in the presence of a source of light energy and an oxidizing agent such as oxygen. In heterogeneous photocatalysis, the interaction of the semiconductor with the light results in the generation of electron-hole pairs. When the light illuminated semiconductor with energy equal to or greater than the band gap, the electrons are moved from a valence band to a conduction band and left behind holes in the valence band. These electron-hole pairs play a role in the degradation of organic dyes, Figure I.11.

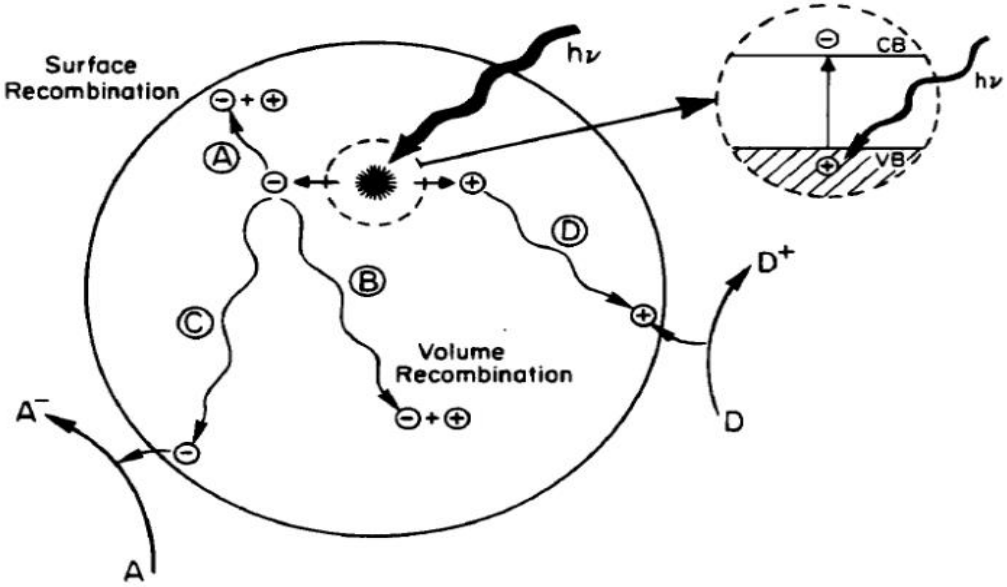

Figure I.11: Diagram of photo excitation in a semiconductor photocatalyst followed by excitation pathways [37].

The electrons of the conduction band of the excited state and the holes of the valence band can then follow several paths [37]. The transfer of photo induced electrons to adsorbed organic or inorganic species or to the solvent results from the migration of electrons and holes to the surface of the semiconductor. At the surface, the semiconductor can give electrons to reduce an electron acceptor (usual oxygen in an aerated solution) (pathway C), a hole can migrate to the surface where an electron from a donor species can be combined with the oxidizing surface hole of the donor species (pathway D).

The probability and rate of charge transfer processes for electrons and holes depend on the position of the band edges for the conduction and valence bands and the redox

potential levels of the adsorbed species. The main challenge of charge transfer to adsorbed species is the recombination of electrons and holes. The recombination of the separated electron and hole may occur in the volume of the semiconductor particle (pathway B) or at the surface (pathway A) and be in the form of heat releasing.

In the heterogeneous photocatalytic process, the reaction itself takes place in the adsorbed phase and the overall process can be decomposed into five independent steps [38]:

- Mass transfer of reagents in the liquid phase to the catalyst surface.
- Adsorbing the reagents on the surface of the photon-activated catalyst.
- The photocatalytic reaction for the adsorbed phase at the catalyst surface.
- Desorption of products from the catalyst surface.
- Desorption of the products from the surface of the catalysts.

I.9.1.4 Semiconductor photocatalysis:

Photocatalyst semiconductors are essentially wide bandgap semiconductors.

Since Fujishima and Honda reported in 1972 the water splitting into H2 and O2 using titanium dioxide (TiO2) electrode [39], semiconductor-based photocatalysis has garnered considerable attention because of its application potential in wastewater treatment and the production of hydrogen fuel using solar or ultraviolet light. P-type semiconductors are rarely used in photocatalytic semiconductors and generally, only n-type semiconducting oxides are used. ZnO, NiO, Fe2O3, tungsten oxide (WO3) are the best known of semiconductor photocatalysis but their photocatalytic activity is lower than that of titanium dioxide (TiO2) which is the most useful photocatalyst for the environmental application.

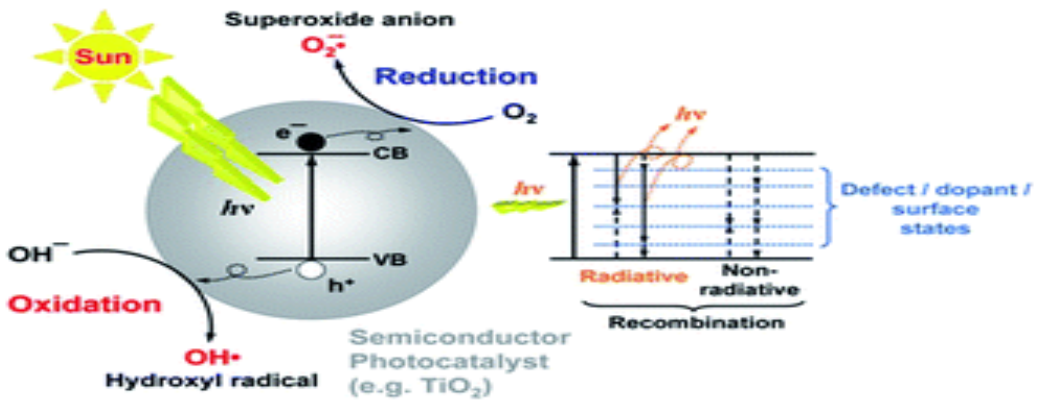

Figure I.12: Schematic of semiconductor photocatalysis process [37].

Therefore, the photons must have high energies to generate electrons from the valence band to the conduction band. In general, these photons belong to the UV part.

There are many approaches to obtain semiconductor with a photocatalytic activity under solar radiation and different photocatalytic systems were used.

We intend to use the systems shown in figure I.13 (b).

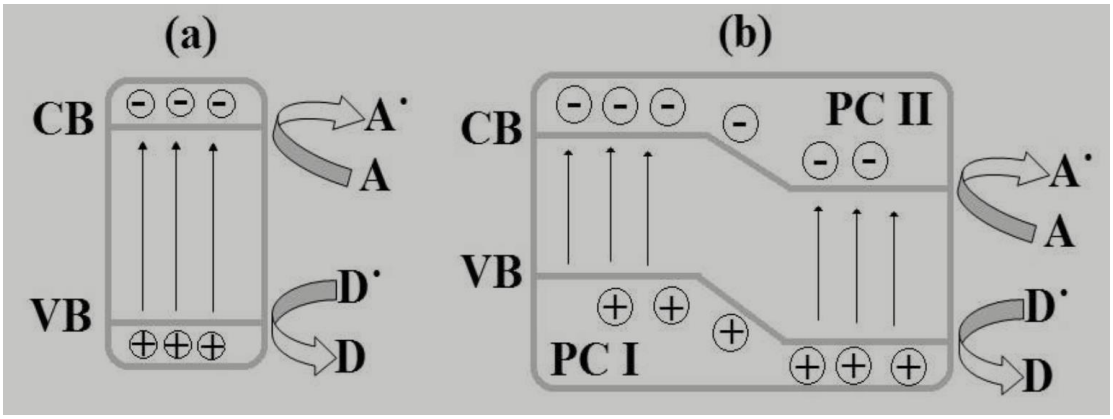

Figure I.13: Schematic diagrams of photocatalytic systems.

a) Single photocatalyst, (b) type II heterojunction. (PC I: photocatalyst I, PC II: photocatalyst II) [39].

In general, studies focus on the development of efficient photocatalytic materials and attempt to obtain the following characteristics [40]:

- High-efficiency photocatalysts which absorb a large amount of solar energy (ability to generate electron-hole pairs).
- High charge separation (electron-hole pairs).
- Less expensive and easier to produce, non-toxic and durable.

I.10 Conclusion:

Through this chapter, we defined the thin film. Then we presented general properties of Nickel oxide. At the end of the chapter we explained some metal oxide application and we focused on Solar cells, photodetectors and photocatalysis.

Materials sciences and Engineering

CHAPTER 2: METHODES OF DEPOSITION AND CHARACTERIZATION

II.1.Introduction:

As it has been discussed in the chapter one, the study of iron oxide is motivated because of its intrinsic physicochemical properties but also due to its low-cost and non-toxic when compared with other materials.

This chapter contains the different methods of the deposition thin films include a description of the chosen deposition procedures and the techniques used to characterize thin films.

II.2.Thin film deposition methods:

The processes for producing thin films are divided into two types, the physical and the chemical methods. The broad classification of deposition techniques is outlined in the figure II.1. An enormous number of deposition processes that exist and just only some methods are detailed in the next part with special emphasis on our processes "the spray pyrolysis method"

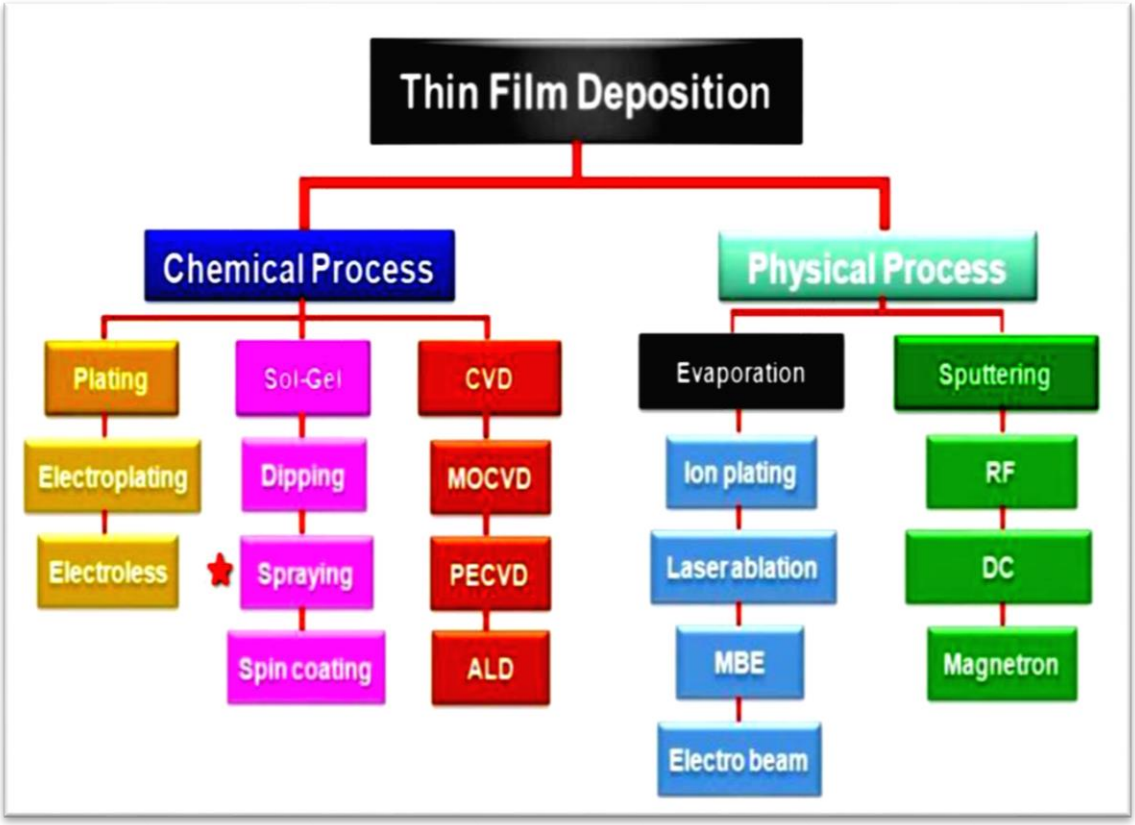

Figure II.1: Schematic diagram of classifications of thin films deposition techniques [41].

II.3.Criteria for selection of deposition methods:

The selection of a specific technology for the deposition of thin films can be based on a variety of considerations. A multitude of thin films of different materials can be deposited for a large variety of applications; hence, no general guidelines can be given of what the most suitable deposition technology should be. In selecting an appropriate deposition technology for a specific application, several criteria have to be considered. In order to optimize the desired film characteristics, a good comprehension of the advantages and restrictions applicable to each technique is necessary. The choice of a specific deposition technique related to some factors, they are:

- The material to be deposited.
- The rate of deposition.
- Limitations imposed by the substrate, e.g.: maximum deposition temperature.
- Adhesion of the deposits to a substrate.
- Throwing power.
- The purity of target material.
- Availability of the required equipment.
- Cost.
- Ecological considerations.
- The abundance of the material (to be deposited).

II.4.Different deposition techniques:

The properties and versatility of the thin films can be obtained by selecting proper technique of film deposition. Thin film deposition methods can be broadly classified as either chemical or physical methods. The difference between the chemical and physical thin film deposition methods depends upon the method of depositing thin film material on the substrate. In chemical deposition technique, fluid precursor is used which chemically react with the substrate. Since the thin film material is conducted through the fluid precursor, physical deposition is conformal approaching the substrate without preference to a particular direction. A conformal is an uneven interface with the body and has a constant thickness on horizontal and vertical surfaces [47].

II.4.1.Physical vapor deposition (PVD) :

Physical Vapor Deposition (PVD) mainly includes evaporation, spraying in all its forms and laser ablation. The most widely used PVD methods are molecular beam epitaxy, cathodic sputtering.

1. Sputtering:

Sputtering is a technique used to deposit different materials such as metals, refractory materials, dielectrics, and ceramics. The principle of this technique is the bombardment of the material to be deposited (target) by neutral gas ions generally argon, under the effect of bombardment atoms torn from the target and deposits on the substrate located in front of the target. If the atmosphere (gas) of the discharge is chemically neutral, the sputtering is called simple. However, if it consists of active gases such as oxygen O_2 or nitrogen N_2, sputtering is said to be reactive. The basic scheme of operation of the sputtering is shown in figure II.2.

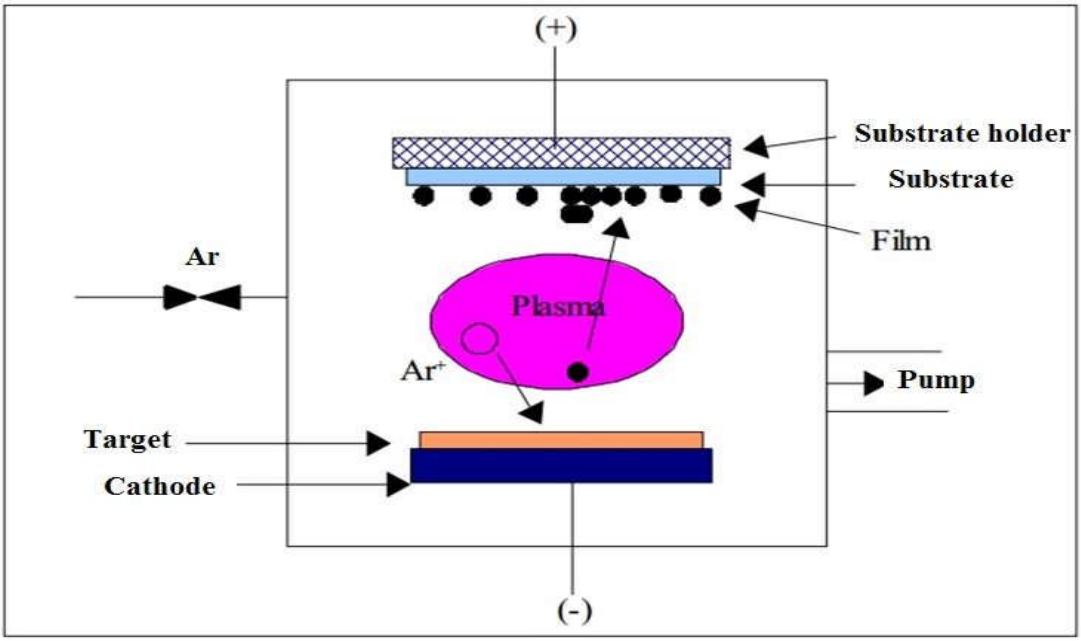

Figure II. 2: The operating principle of sputtering [41].

There are two types of cathodic sputtering depending on the mode of creation of the plasma or the nature of the target (conductive or insulating): direct cathodic sputtering (DC) only in the case of the sputtering of conductive materials and sputtering radiofrequency (RF) which allows the spraying of conductive materials or insulating materials. There are many parameters that affect the deposition process such as base vacuum, sputter gas pressure during deposition, sputter power, target and

substrate temperature, etc…The magnetron device has been used to limit the disadvantages and increase the efficiency of the sputtering.

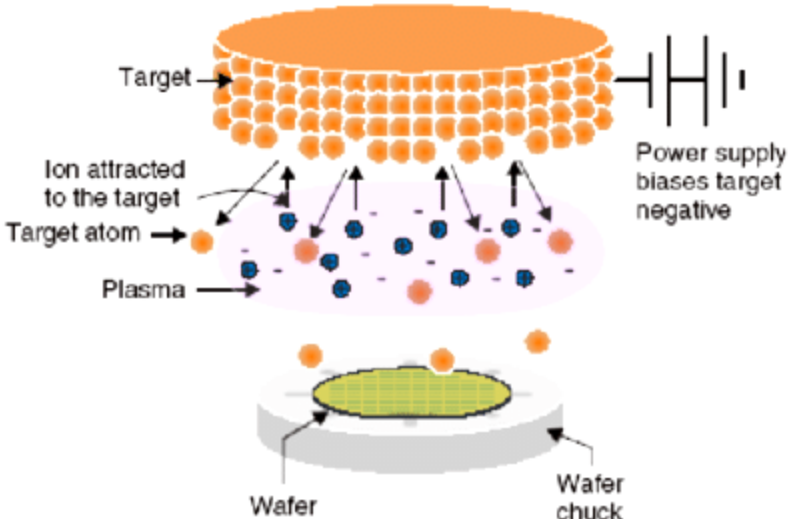

Figure II.3: Cathodic sputtering: accelerated Ar + ions extract atoms from the target [42].

2. Molecular Beam Epitaxy (MBE):

Epitaxy is a compound of two Greek words Epi = on, Taxi = arrangement. It is defined as the formation of a monocrystalline layer called (the epitaxial layer) on a monocrystalline substrate [43].

Molecular beam epitaxy is a method for developing thin films at low temperature with excellent crystalline quality and very low roughness in a very high vacuum (<10-10 Torr). The principle of this technique, Figure II.4, is based on the reaction of atomic or molecular fluxes on a monocrystalline substrate which brought to an adequate temperature [44].

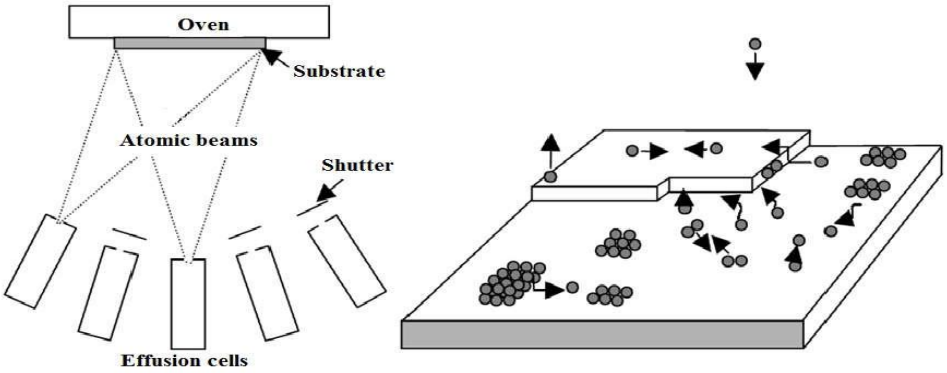

Figure II. 4: The operating principle of MBE [44].

As shown in figure II.4, the growth process of the molecular beam epitaxy can be summarized in the following steps [44]:

1) Deposition of atoms onto the surface of the substrate
2) Nucleation process (creation of di-atomic islands)
3) Growth of islands by coalescence
4) Formation of a layer by coalescence of islands

Molecular beam epitaxy has the following advantages [43]:

- The low growth rate that allows doping at the atomic level
- Possible controls and in situ analysis (RHEED; Auger XPS)
- Very precise control of the thicknesses of the thin layers
- The ability to control all the steps automatically
- No boundary layer.

3. Pulsed Laser Deposition:

Pulsed Laser Deposition (PLD) is a deposition technique that has the advantage of transferring the stoichiometry of the target to the prepared layer, in this method a laser beam focused on a depositing material (target) placed in an ultrahigh vacuum chamber. Under the effect of this laser beam, an amount of the material is pulled away from the target in the form of a dense and light vapor (plasma) and deposited on the substrate placed opposite as presented in figure II.5.

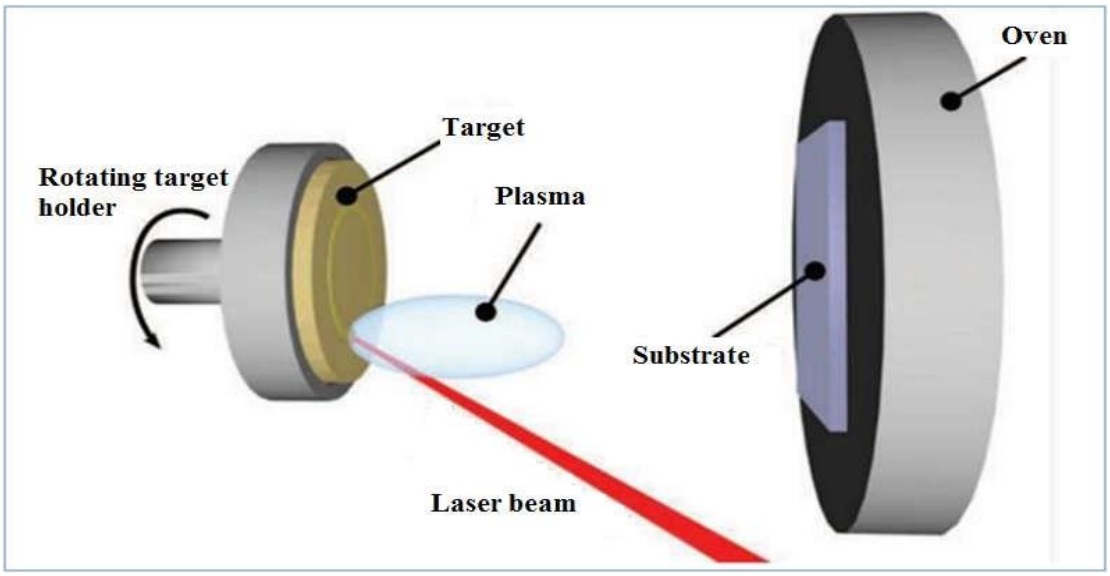

Figure II. 5: Schematic diagram of the Pulsed Laser Deposition (PLD) technique [46].

Laser ablation has a number of advantages, it enables the deposition at room temperature and the coating of all types of the substrate [46], and it also allows the manufacture of the complex composition of materials in thin layers.

4. Thermal evaporation:

The thermal evaporation process contains evaporating source materials in a vacuum chamber below 10-6 Torr and condensing the evaporated particles on a substrate. In this process, thermal energy is provided to a source from which atoms are evaporated for deposition in the substrate. Heating of the source material can be finished by any of which the material to be evaporated is attached. Larger volumes of source material can be heated in crucibles of refractory metals, Oxides or Carbon by resistance heating, high-frequency induction heating, or electron beam evaporation. The evaporated atoms travel through reduced background pressure in the evaporation chamber and condense on the growth surface. The deposition rate or flux is a function of the travel distance from the source to the substrate, the angle of impingement onto the substrate surface, the substrate temperature Ts, and the base pressure. The conventional thermal evaporation system is mentioned in figure II .6 [47-48].

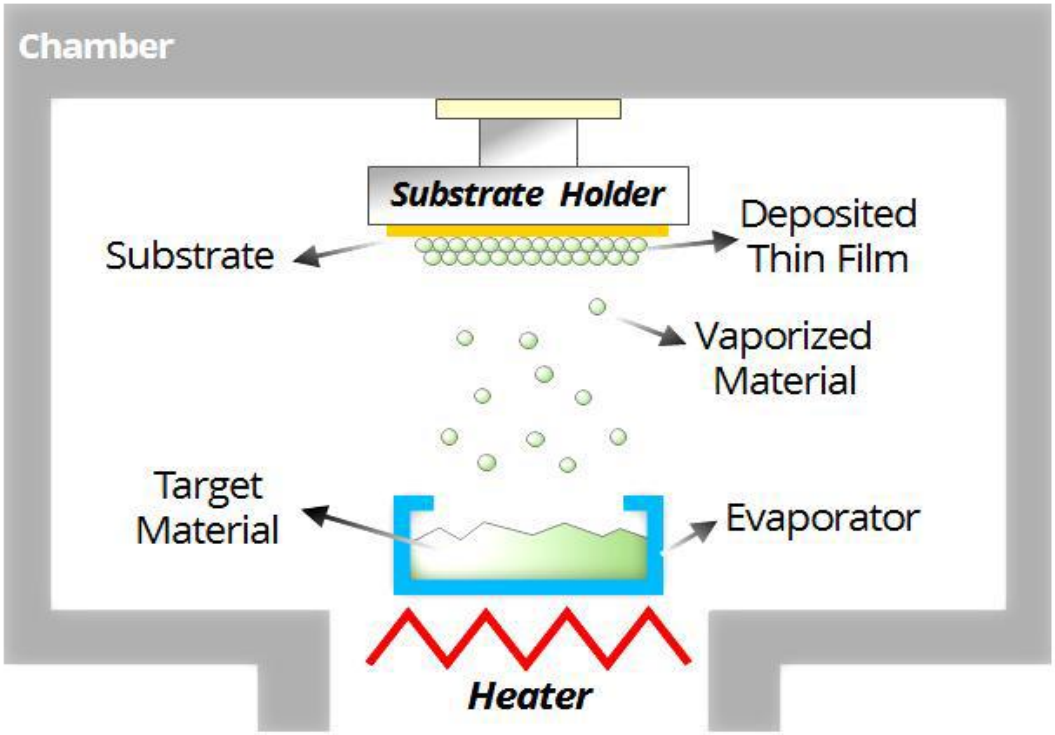

Figure II .6: Schematic diagram of thermal evaporation system [49].

II.4.2.Chemical deposition:

1. Chemical Vapor Deposition (CVD):

The CVD technique consists of developing materials in the form of thin layers from gaseous precursors that chemically react to form these layers on a heated substrate [45], as shown in figure II.7. The CVD process can be summarized in five steps [44]:

- Transporting reactive gas species (or species) to the substrate.
- Adsorption of the reactants on the surface.
- Surface reaction and film growth.
- Desorption of volatile secondary products.
- Transport and evacuation of gaseous products to the reactor outlet.

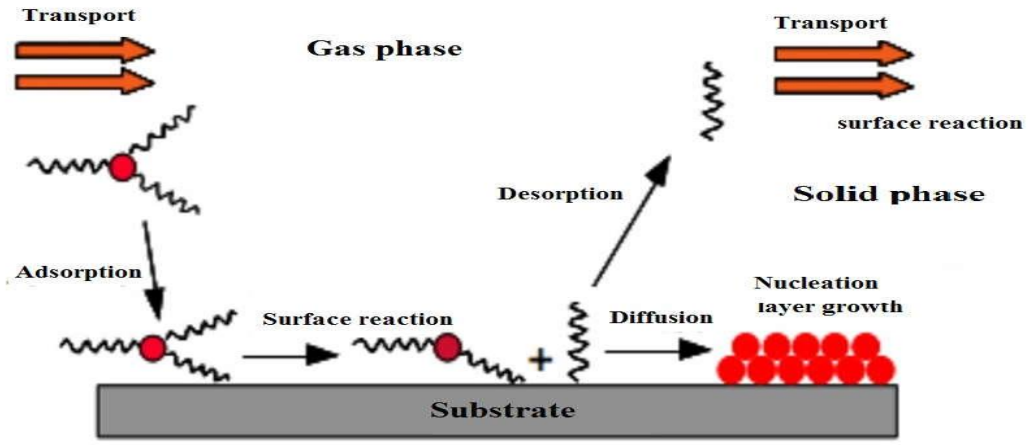

Figure II.7: Schematic diagram of thermal evaporation system [43].

The improvement of this technique is to reduce the deposition temperature and the reactor pressure and remedy the low volatility of the precursors. Several CVD type techniques can be given [51]:

- APCVD: (Atmospheric Pressure Chemical Vapor Deposition) deposition under atmospheric pressure.
- LPCVD: (Low-Pressure Chemical Vapor Deposition) low-pressure deposition.
- MOCVD: (Metal Organic CVD) the use of organometallic precursors.
- PACVD: (Plasma Assisted Chemical Vapor Deposition) with the assistance of a plasma.

2. Sol-Gel:

The term sol-gel corresponds to the abbreviation "solution-gelation". The sol-gel method, figure II.8, used to manufacture various materials such as ceramics, powders, fibers, and thin films and is particularly well suited for producing coatings such as thin layers of oxides [52, 53].Its principle is based on chemical reactions of a chemical precursor consisting of metal atoms of the material that we want to deposit in a solution to form an oxide network at an infinite viscosity called "gel", depending on the nature of the precursors used. We distinguish two synthetic voices [54]:

Inorganic route: obtained from metal salts such as nitrates, sulfates, chlorides, or acetates; dissolved in an aqueous solution.

Organometallic route: The most frequently used precursor is metal alkoxides in organic solutions.

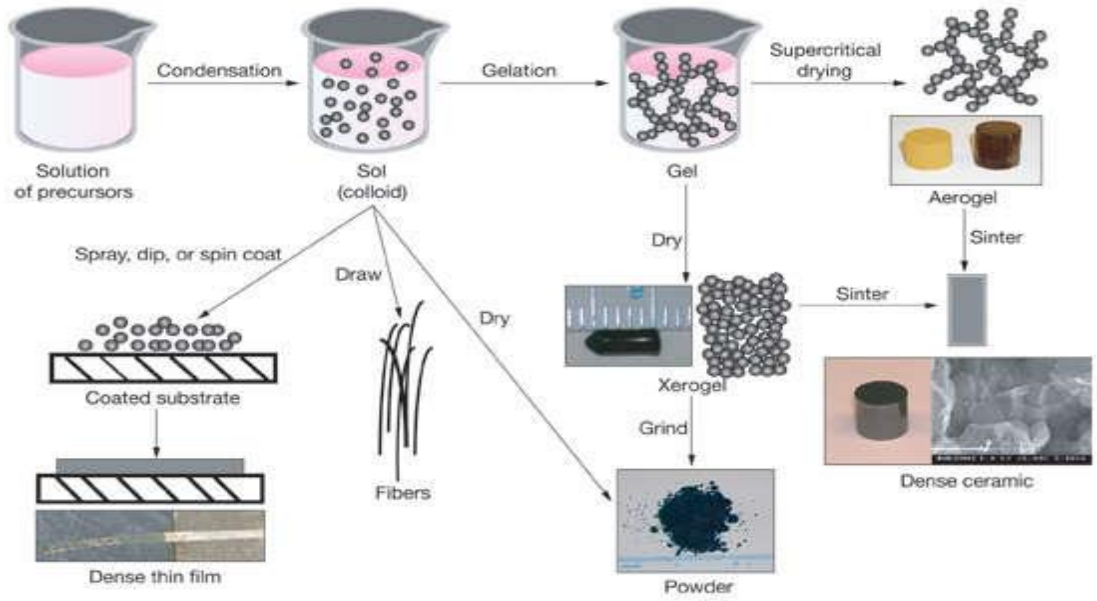

Figure II.8 Synthesis of various forms of materials by the sol-gel method [55].

3. Chemical bath deposition:

The chemical bath deposition (CBD) is also recognized as controlled precipitation; it has been applied since to deposit films of many different semiconductors. It is currently attracting great attention as it does not necessitate sophisticated instrumentation like vacuum system and other expensive equipment. All that is required is a vessel to include the solution (an aqueous solution made up of a few usually common, chemicals) and a substrate on which deposition is required. It offers

a bottom-up approach to prepare nano-crystalline materials in thin film form with better particle size controlled, particle shape, size distribution, particle composition, the degree of particle agglomeration, the conventional thermal evaporation system is presented in figure II.9 [56].

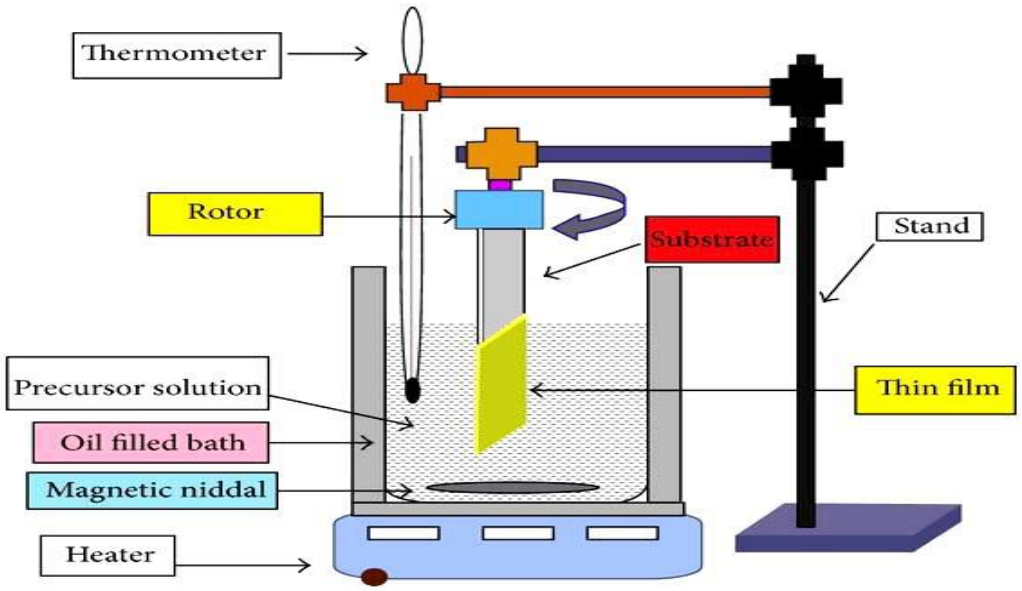

Figure II.9: Schematic diagram of chemical bath deposition system [56].

4. Chemical Spray Pyrolysis Technique:

Numerous materials have been prepared in the form of thin film because of their potential technical value and scientific curiosity in their properties. A number of techniques have been examined in the search for the most reliable and cheapest method of producing thin films [57]. Chemical spray pyrolysis (CSP) technique was initially suggested by Chamberlin and Skarman in 1966 to prepare CdS (*Cadmium sulfide***)** thin films on glass substrates. This method was used by many workers [58- 59]. Spray pyrolysis involves spraying of an aqueous solution containing soluble salts of the constituent atoms of the desired compounds to the heated substrates. The liquid droplets vaporize before reaching the substrate or react on it after splashing [60]. Doped and mixed films can be prepared very easily, simply by adding to the spray solution a soluble salt of the desired dopants or impurity.

The principle of deposition thin film from the spray pyrolysis method requires heated substrate in order to spray the metal salt from the aqueous solution. Droplets were scattered and formed a disk-shaped structure into the surface of the substrate and undergo thermal decomposition.

The size and shape of the disk correlated with substrate temperature, the volume, and momentum of the droplet. Consequently, this film was produced and included overlapping disks of metal salt being changed to metal oxide. Some types of spray pyrolysis devices are developed to exploit the capability of the technique coupled with the properties of the solution precursors. The change in atomization method resulted in different spray pyrolysis techniques. They are [61]:

- Pressurized air blast (liquid is exposed to a stream of air).
- Ultrasonic wavelengths were produced and are required for fine atomization.
- Electrostatic (liquid interacts with the existence of high electric field).

Out of all these, pressurized air blast spray deposition is the most simple and cost effective.

The spray parameters can be very well controlled. The fundamental of spray pyrolysis components is spray nozzle, a rotor for a spray nozzle, liquid level monitor, hot plate, gas regulator valve and air compressor as it mentioned in figure II.10.

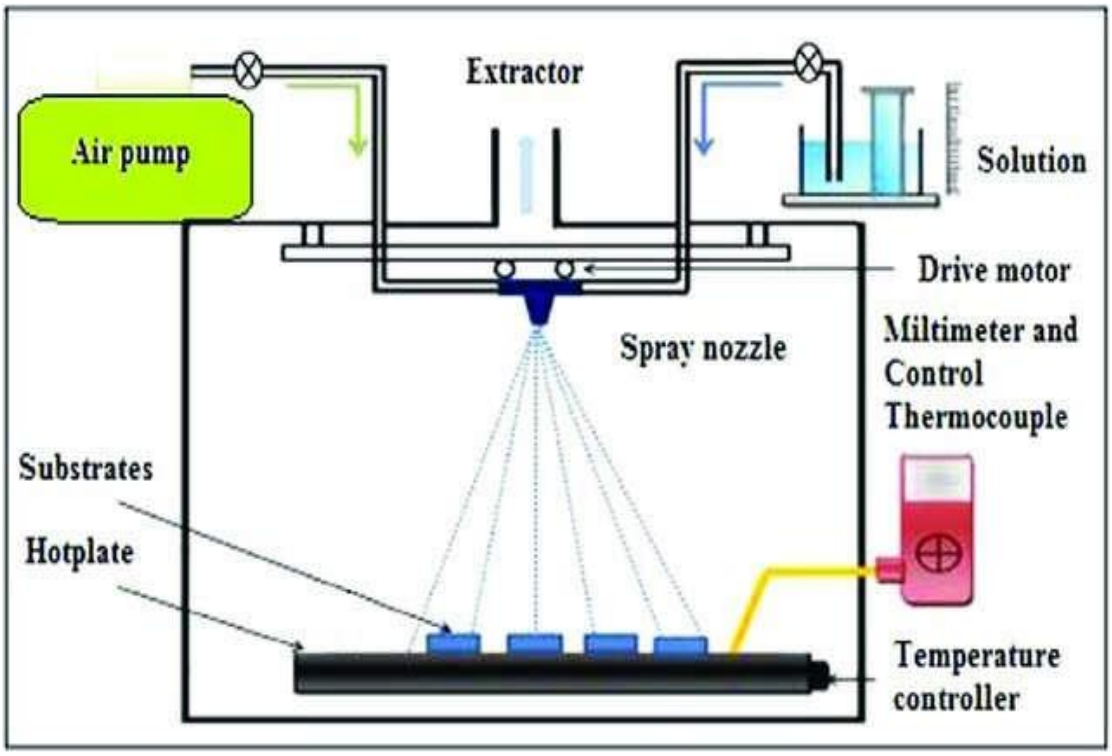

Figure II.10: Schematic of spray pyrolysis technique [58].

In spray pyrolysis, the experimental parameters such as precursor solution, decomposition of the precursor, atomization, and aerosol transport are very significant in order to examine the structural, compositional, surface topology, electrical and optical properties of the thin films.

The parameters that influence the properties of the thin layers prepared by spray pyrolysis are [62-63]:

- The temperature of the substrate.
- The precursor solution (the type of solvent, the viscosity of the solution, the concentration of the compound in the solution).
- The distance between the nozzle and the substrate.
- The carrier gas and the rate at which the aerosol passes through.
- The size and opening time of the nozzle.
- The number of sprays.

Chemical spray pyrolysis technique has a number of advantages as depicted in the following points [64, 65]:

1. It offers an extremely easy way to dope films with virtually any element in any proportion by merely adding it in some form to the spray solution.

2. Unlike closed vapor deposition method, CSP does not require high quality targets and/or substrates, and it does not require vacuum at any stage, which is a great advantage if the technique is to be scaled up for industrial applications.

3. The deposition rate and the thickness of the film can be easily controlled over a wide range by changing the spray parameters, thus eliminating the major drawbacks of chemical methods such as sol-gel method which produces films of limited thickness.

4. Operating at moderate temperatures (100 – 500^{o}C), CSP method can produce films on less robust material.

5. Unlike high – power methods such as radio frequency magnetron sputtering (RFMS), it does not cause local over – heating that can be detrimental for materials to be deposited.

6. By changing composition of the spray solution during the spray process, it can be used to make layered film having composition gradients throughout the thickness.

7. It is believed that reliable fundamental kinetic data are more likely to be obtained on particularly well characterized film surface, provided the film are quiet compact, uniform and that no side effects from the substrate occur. CSP offers such an opportunity.

8. Low cost comparing with other methods which require complex devices and instruments with high cost.

II.5.Films characterization techniques:

Characterization techniques recently nanostructured semiconducting materials are synthesized by different physical and chemical methods. The structural and electronic properties as well as the primary particle size distribution are strongly dependent on the preparation method. Once the synthesis of an appropriate material is done, the first goal is to perform the characterizations of that particular material. In order to perform this in a systematic way, one needs a diverse array of characterization techniques. [66] An important issue is the correct interpretation of the experimental results obtained by characterization tools. To confirm this, in this element we will describe the various characterization techniques may utilized in our work.

1. Weight difference method.
2. X-Ray diffraction technique (XRD): for the study of structural properties.
3. Scanning electron microscopy (SEM).
4. Ultra-violet-visible spectroscopy (UV-Vis): for the study of optical properties.
5. Method of four probes: for the study of electrical properties.

II.5.1.Weight difference method:

Film thickness is one of the very important attributes of the films to be determined. The reason is that many properties of the films are dependent on the film thickness and other parameters such as mass density can be derived from thickness.

There are various methods to measure the film thickness, among them optical method (Hebal Optics) and weight difference method. The weight difference method is simple and available only need a precise electronic balance, the thickness is measured in this method using the following formula [67]:

$$t(nm) = \frac{\Delta m}{S\, n} \qquad \text{(II.1)}$$

Where (t) is the thickness of the film, (Δm) is the weight gain, (S) is the area of the coated film and (η) is the density of NiO in bulk state.

II.5.2.X-Ray diffraction technique :

(XRD) is one of the most useful characterization methods as it can provide a great deal of information about the film without requiring much sample preparation.

X-ray diffraction can be used to study the crystallographic properties of the thin films prepared such as determine of the crystalline structure, the orientation of the crystallites in a sample, the crystalline quality and the crystallite sizes. Two critical advantages of X-ray diffraction for thin film analysis are [68]:

1. The wavelengths of X-rays are of the order of atomic distances in condensed mater, which especially qualifies their use as structural probes.

2. X-ray scattering techniques are non-destructive and leave the investigated sample intact.

X-ray diffraction has been used to identify the crystalline phases of the materials based on the Bragg's law. As shown in figure II.11**,** condition at which diffraction occurs in a crystalline material satisfying the Bragg's law is described as [69]:

$$n\lambda = d_{hkl} \sin(\theta_{hkl}) \qquad \text{(II.2)}$$

Where (λ) is the wave length of the X-ray beam, (d_{hkl}) is the spacing between the parallel planes in the atomic lattice, (*h, k and l*) are the miller indices of the corresponding lattice planes (*hkl*), θ_{hkl} is the angel between the incident ray and the scattering planes, and *n* is an integer. Waves that satisfy this condition interfere constructively and result in a reflected wave of significant intensity.

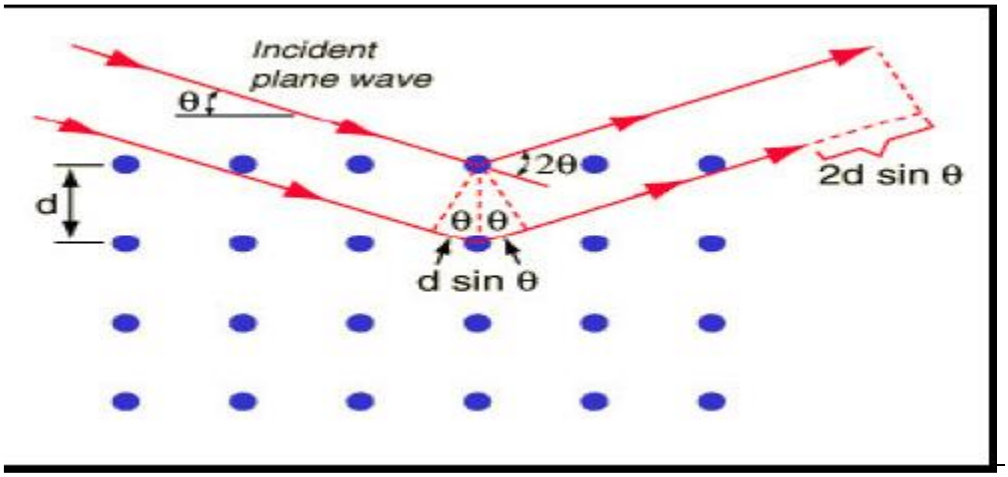

Figure II.11: Schematic of X-ray diffraction According to Bragg. [69]

A diffraction pattern is obtained by measuring the intensity of scattered waves from a sample as a function of scattering angle.

Very strong intensities known as Bragg peaks are obtained in the diffraction pattern at the points where the scattering angles satisfy Bragg condition.

X-ray diffraction studies give a whole range of information about the crystal structure, orientation and average crystalline size of the films.

The diffraction patterns obtained experimentally of the sample are compared with the standard patterns of the likely elements and compounds present in the sample. Based on this comparison conclusions can be drawn about crystal structure and orientation of the sample.

Information obtained from the X-ray Diffractogram:

There is much information that we can deduce from the X-ray Diffractogram, some of which are presented below.

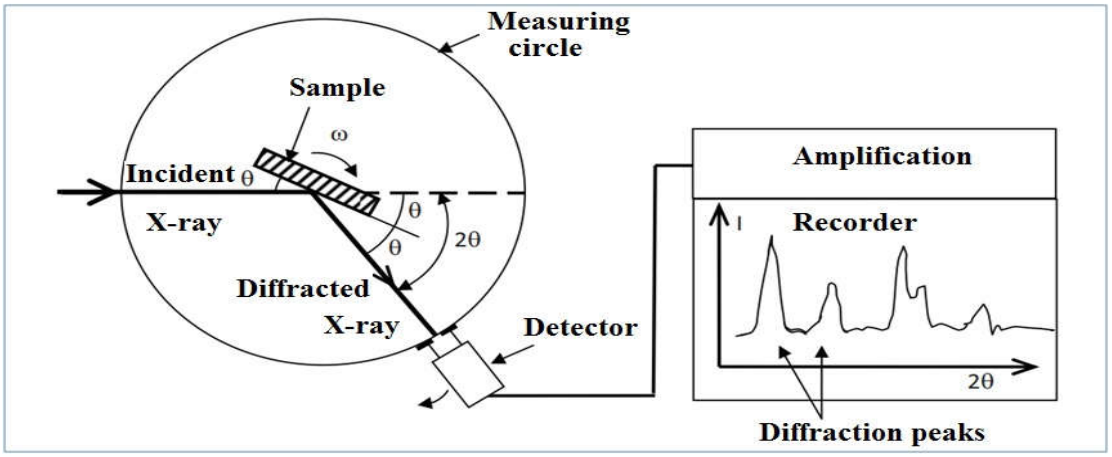

Figure II.12: Schematic diagram of an X-ray diffractometer [40].

A. grain size:

From the X-ray diffraction pattern, the width generated in a peak which known as full width at half maximum (FWHM) (figure II.13), can be used to calculate the mean crystallites sizes of the film in a direction perpendicular to the respective (*hkl*) planes, by using the Scherer's formula [70, 71], which is given as:

$$D_{hkl} = \frac{0.9\lambda}{\beta_{hkl}\cos(\theta_{hkl})} \qquad \text{(II.3)}$$

Where (D_{hkl}) is the average grain size obtaining from the peak (*hkl*), (λ) is the wave length of the X-ray beam, (β_{hkl}) is the full width at half maximum intensity of the peak (*hkl*) and (θ_{hkl}) is the angel between the incident ray and the (*hkl*) scattering planes.

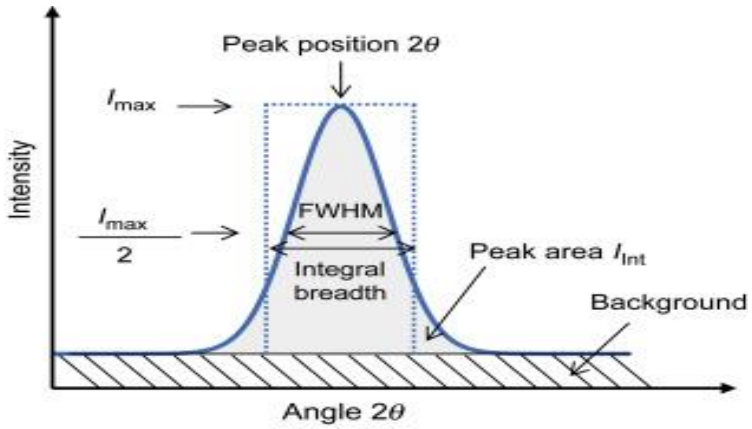

Figure II.13: Full width at half maximum (FWHM) of an arbitrary peak [71].

B. Lattice parameters:

Experimentally, the Bragg law can be utilized by using X-rays of known wavelength (λ_0) and measuring (θ_{hkl}^{exp}), we can determine the inter planar spacing (d_{hkl}^{exp}) of various planes in a crystal.

$$d_{hkl}^{exp} = \lambda_0 / 2\sin\theta_{hkl}^{exp} \qquad \text{(II.4)}$$

Lattice Constant (a_o) can be calculated of a particular cubic system through the following relation. (hkl) parameters and the inter planar spacing (d_{hkl}^{exp}) [72].

$$d_{hkl}^{exp} = \frac{a_{hkl}^{exp}}{\sqrt{h^2 + k^2 + l^2}} \qquad \text{(II.5)}$$

The lattice parameters are substrate dependent. This gives rise to a mismatch between the substrate and the deposited thin films. The latter is responsible of the resulting strains and stresses.

The strain (ε) values of the films were estimated from the observed shift, in the diffraction peak between their positions in the XRD spectra via the formula [73, 74]:

$$\varepsilon = (a_{hkl}^{exp} - a_{hkl}^{the}) / a_{hkl}^{the} \qquad \text{(II.6)}$$

Where (ε) is the mean strain in thin films, a_{hkl}^{exp} is the lattice constant of thin films and a_{hkl}^{the} the lattice constant of bulk.

We can be also estimating the lattices micro strain (μ_ε) using another relationship [75, 76]:

$$\mu_\varepsilon = \beta \cos(\theta)/4 \quad \text{(II.7)}$$

A dislocation is an imperfection within the crystal associated with the miss registry of the lattice in one part of the crystal with that in another part. Unlike vacancies and interstitial atoms, dislocations are not equilibrium imperfections, i.e. thermodynamic considerations are insufficient to account for involving dislocation as a matter of importance [77]. The dislocation density (δ) is the dislocation lines per unit area of the crystal can be evaluated from the grain size (*D*) using the formula [76, 78]:

$$\delta = 1/D^2 (Lines/m^2) \quad \text{(II.8)}$$

C. Texture:

To describe the preferential orientation, the texture coefficient, TC (*hkl*) is calculated.

$$TC(hkl) = \frac{I(hkl)/I_0(hkl)}{\frac{1}{N}\sum_N I(hkl)/I_0(hkl)} \quad \text{(II.9)}$$

Where *I* (hkl) is the measured intensity of a plane (hkl), I_0 (hkl) is the standard intensity of the plane (hkl) taken from the JCPDS data and *N* is the number of diffraction peaks. The value TC (*hkl*) =1 represents films with randomly oriented crystallites, while higher values indicate the abundance of grains oriented in a given (hkl) direction [79].

. Values 0< T*C(hkl)* <1 indicate the lack of grains oriented in that direction. As *TC(hkl)* increases, the preferential growth of the crystallites in the direction perpendicular to the *hkl* plane is the greater [79].

D. Dislocation density and number of grains:

The dislocation density (δ) can be calculated as the following [79]:

$$\delta = 1/D_{av}^2 \quad \text{(II.10)}$$

and number of crystallites can be calculated from the relation [79]:

$$N_0 = t/D_{av}^3 \quad \text{(II.11)}$$

Where t: is the thickness and N_0: is the number of crystallites.

II.5.3.Scanning electron microscopy (SEM):

The scanning electron microscope (SEM) is a multipurpose and commonly employed electron beam mechanism. Its reputation in scientific world developed from its simple interpretation methods of the generated micrographs, variety of information types that it can produce and combination of images with their analytical information counterpart [80, 81]. SEM's are used for material characterization involving image and quantitative data representation. It offered an insight into the two dimensional and three dimensional imaging of the microstructure, chemical composition, crystallography and electronic properties. Light microscopes (LM) operate using light to illuminate the surface to observe the structure; this limits resolution of these microscopes to the wavelength of light. Optical microscopes generally observe an optical limit around 300nm, whereas electron microscopes (EM) offer atomic resolution [81].

A schematic representation of a typical SEM is shown in figure II.14 Electrons emitted from an electron gun pass through a series of lenses to be focused and scanned across the sample. Electron beams having energies ranging from 0.5 keV to 30 keV, is focused by one or two condenser lenses. The beam then passes through pairs of scanning coils or pairs of deflector plates in the electron column, typically in the final lens.

When the electron beam interacts with the sample, the electrons lose energy by repeated random scattering and absorption. The energy exchange between the electron beam and the sample results in the reflection of high-energy electrons by elastic scattering, emission of secondary electrons by inelastic scattering and the emission of electromagnetic radiation, each of which can be detected by detectors. The beam current absorbed by the specimen can also be detected and used to create images of the distribution of specimen current. Electronic amplifiers of various types are used to amplify the signals, which are displayed as variations in brightness on a cathode ray tube (CRT) [81, 82]. The raster scanning of the CRT display is synchronized with that of the beam on the specimen in the microscope, and the resulting image is therefore a distribution map of the intensity of the signal being emitted from the scanned area of the specimen. The image can be digitally captured and displayed on a computer monitor and saved to a computer's hard disk.

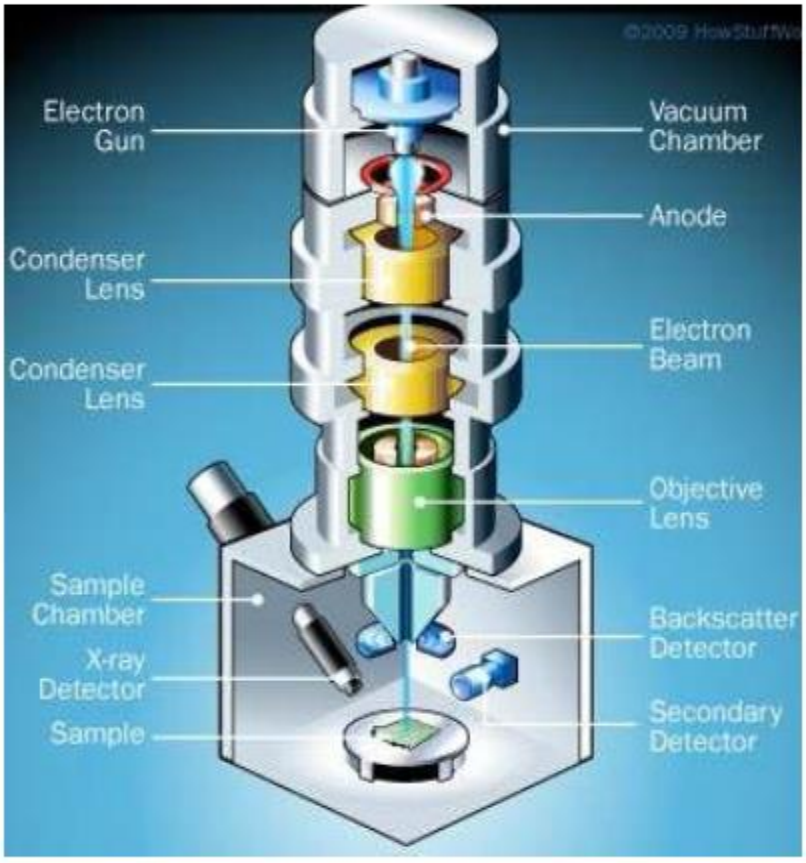

Figure II.14: Schematic representation of scanning electron microscope [83].

II.5.4.Spectroscopy UV- visible:

The thin layers have optical properties interesting for various applications. So, Optical absorption characterization has become an important tool for optically characterizing transparent samples. By way of example, it is strongly used to highlight the effects of quantum confinement induced by the small size of the crystallites. Using a spectrometer it is possible to measure the transmittance, the optical gap, the activation energy, the extinction coefficient, the absorption coefficient. In this work, some parameters of the optical properties of thin films were determined by exploiting curves representing the variation of the transmittance as a function of the wavelength in the field of UV-visible. The operating principle of the device is shown in figure II.15.

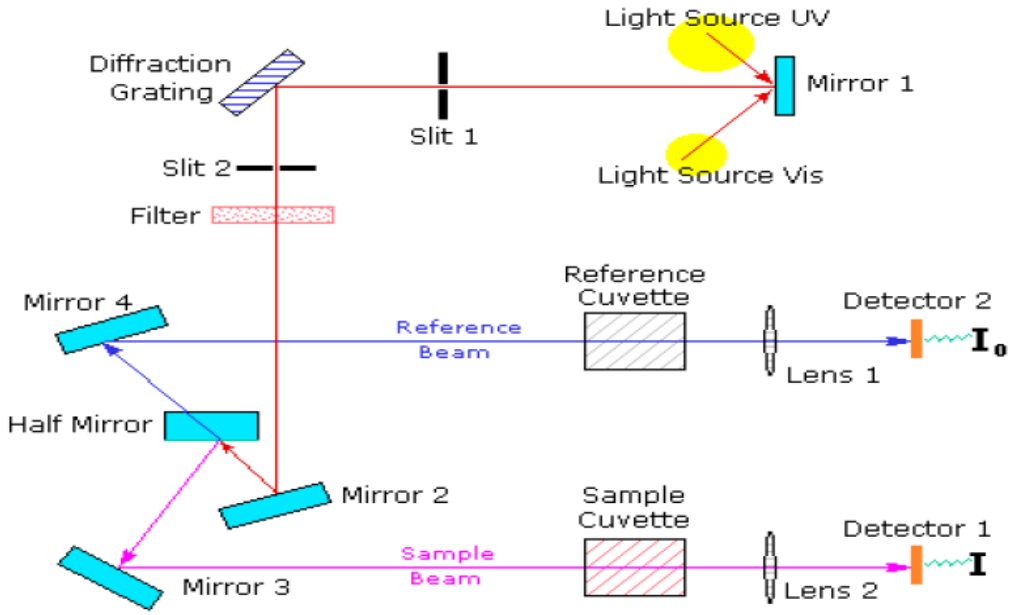

Figure II.15: Schematic representation of UV-Visible spectrometer [84].

When a substance absorbs light in the in the ultraviolet and visible domains, the energy absorbed causes disturbances in the electronic structure of atoms, ions or molecules.

One or more electrons absorb this energy to jump from a low energy level to a high energy level. These electron transitions are in the visible range, from 350 to 800 nm and ultraviolet between 200 and 350 nm. A homogeneous medium traversed by the light absorbs a part of it, the different radiations constituting the incident beam are differently absorbed according to their energies, the transmitted radiations are then characteristic of the medium [85, 86].

The absorption of energy of photon equal or more than the band gap of the semiconductor induces a photo-excitation, while transmittance can be defined as the fraction of light of a given wavelength incident to a material that passes through that material.

Figure II.16 presents the transmission curve of an arbitrary transparent thin film semiconductor. Incident photons with energies $h\nu \geq$ Eg are absorbed, this absorption determined by the properties of the film (e.g. thickness & impurities), since there are numerous valence band electrons and the conduction band contains many empty states into which these electrons can be excited. A photon with energy $h\nu < Eg$ is unable to excite a valence band electron to the conduction band, and as consequence they are transmitted, this explains why some semiconductors are transparent in certain

wavelength ranges. Thus, for pure (intrinsic) semiconductors. There is negligible absorption of photons with $h\nu$ < Eg, a photon will be absorbed only if there are available energy states in the forbidden band gap due to chemical impurities or physical defects, this process is called extrinsic transition [67].

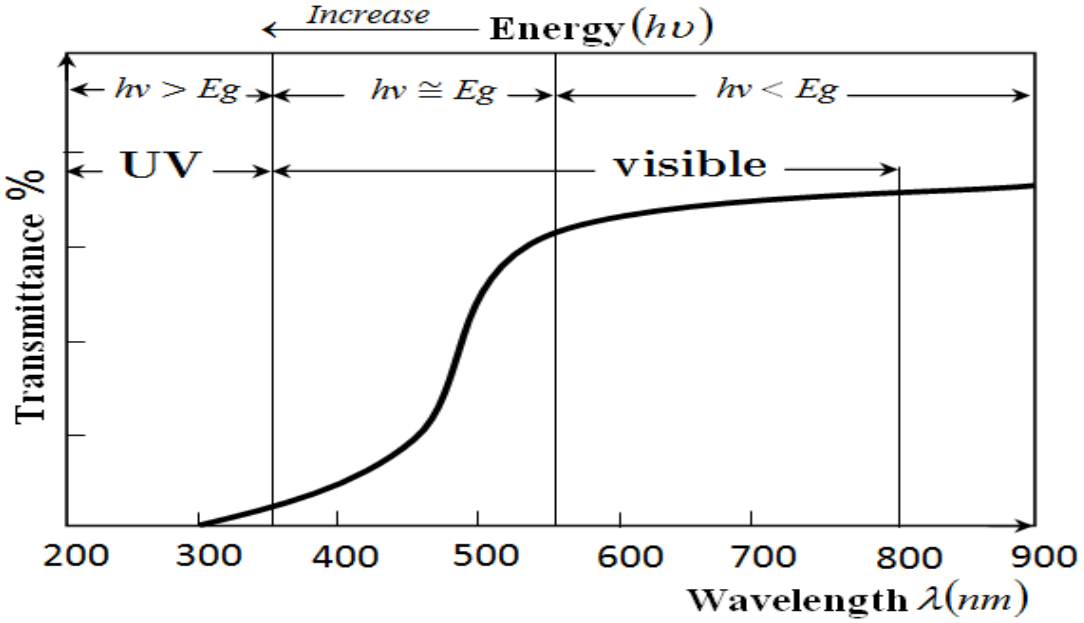

Figure II.16: Presents the transmittance curve of a thin film of metal oxide semiconductor [67].

Information obtained from the UV-Visible transmittance spectra:

Much information is obtained about the properties of materials when they interact with electromagnetic radiation. When the light beam (photons) is an accident on an object, there is some expected absorption, determined by the properties of the material.

In the following we will integrate the properties of films that can be deduced from the transmittance spectrum.

A. Absorption coefficient:

Absorption coefficient expresses the decrease in the intensity of a beam of photons at its passage through a particular substance or medium.

When radiation of intensity (φ_0) is incident on material of thickness (t (*nm*)) the transmitted intensity (ϕ) is given by Lambert-Beer-Bouguer's law [87]:

$$\phi = \varphi_0 \exp(-\alpha t) \qquad \text{(II.12)}$$

For pure absorption, the constant (α) is the absorption coefficient. For scattering, obeying by Lambert-Beer-Bouguer's law, (α) is the scattering coefficient. And for the total attenuation including both is the extinction coefficient given by the sum of the absorption and scattering coefficient.

The transmittance (T) and the absorbance (A) are defined as follows [88]:

$$T = \phi \,|\, \phi_0 = \exp(-\alpha t) \tag{II.13}$$

$$A = -\log_{10}(T) \tag{II.14}$$

A relation between transmittance (T), spectral absorbance (A) and spectral reflectance (R), according to the law of conservation of energy is given by [89]:

$$T + R + A = 1 \tag{II.15}$$

Based on the equations (II.13) we can obtain the following expression of absorption coefficient [88-90]:

$$\alpha = -\frac{\ln(T)}{t} \approx 2.303\frac{A}{t} \tag{II.16}$$

We are using equation (I.14) for calculating the reflectance and equation (II.14) for calculating the absorption coefficient in this work.

For ($h\nu < E_g$), no electron hole pairs can be created, the material is transparent and (α) is small. For ($h\nu > E_g$) absorption should be strong and it is clear that (α) must be strong. The absorption coefficient (α) is related to the incident photon energy (hν) and the optical band gap energy of the material as [67, 90]:

$$(\alpha h\nu) = C(h\nu - E_g)^n \tag{II.17}$$

Where C is a constant is a constant depending upon the transition probability, E_g is the optical band gap, it is shown in figure II.17, it is the separation energy between bottom of the conduction band and top of the valence band. ($h\nu$) is the photon energy, where (ν) is the frequency of the incident photon, (h) is the Planck's constant and (n) is a constant it is equal to 1/2 or 3/2 depending on whether transition is allowed or forbidden. For allowed direct transitions (n =1/2) and for allowed indirect transition (n = 2). Thus if the plot of $(\alpha h\nu)^2$ against $h\nu$ is linear then the transition is direct allowed [87].

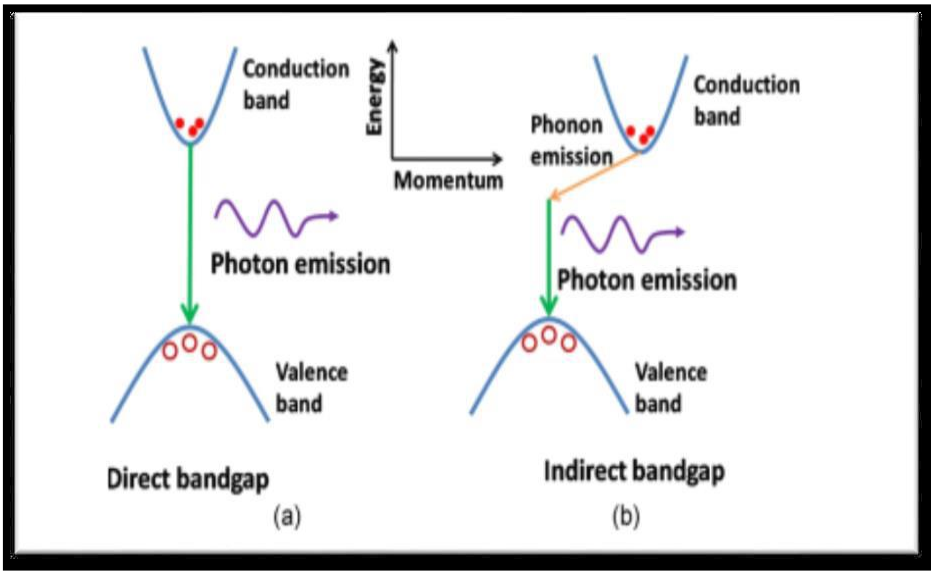

Figure II.17: Direct (a) and indirect (b) band gap [90].

From the calculated absorption coefficient (α) values the extinction coefficient (k*)* of the films were calculated over visible and near infra-red wavelengths using the following formula [91]:

$$k = \frac{\alpha\lambda}{4\pi} \qquad \text{(II.18)}$$

Where λ is the wavelength of the incident photon.

The rise and fall in the extinction coefficient are directly related to the absorption of light. In the case of polycrystalline films, extra absorption of light occurs at the grain boundaries [90].

This leads to non-zero value of k for photon energies smaller than the fundamental absorption edge.

B. Energy band gap:

The energy band gap and transition type can be determined from mathematical treatment of data obtained from optical transmittance versus wavelength. According to Tauc's relation for direct bang gap semiconductor such as NiO [90, 91]:

$$(\alpha h\nu)^2 = A(h\nu - E_g) \qquad \text{(II.19)}$$

Where (*A*) is a constant, (E_g) is the optical gap energy. Figure II.18 shows the plot of $(\alpha h\nu)^2$ versus (hν), it reveals the linear nature of the plot near absorption edge indicates the existence of the direct transition between bands. Hence, this linear relationship is a clear indication that the material is direct band gap semiconductors.

Extrapolating the straight line portion of the absorption spectrum in figure II.18 intersects the zero absorption coefficients (α=0) (energy axes) [92]. The value of energy at this interesting point indicates the energy of band (E_g).

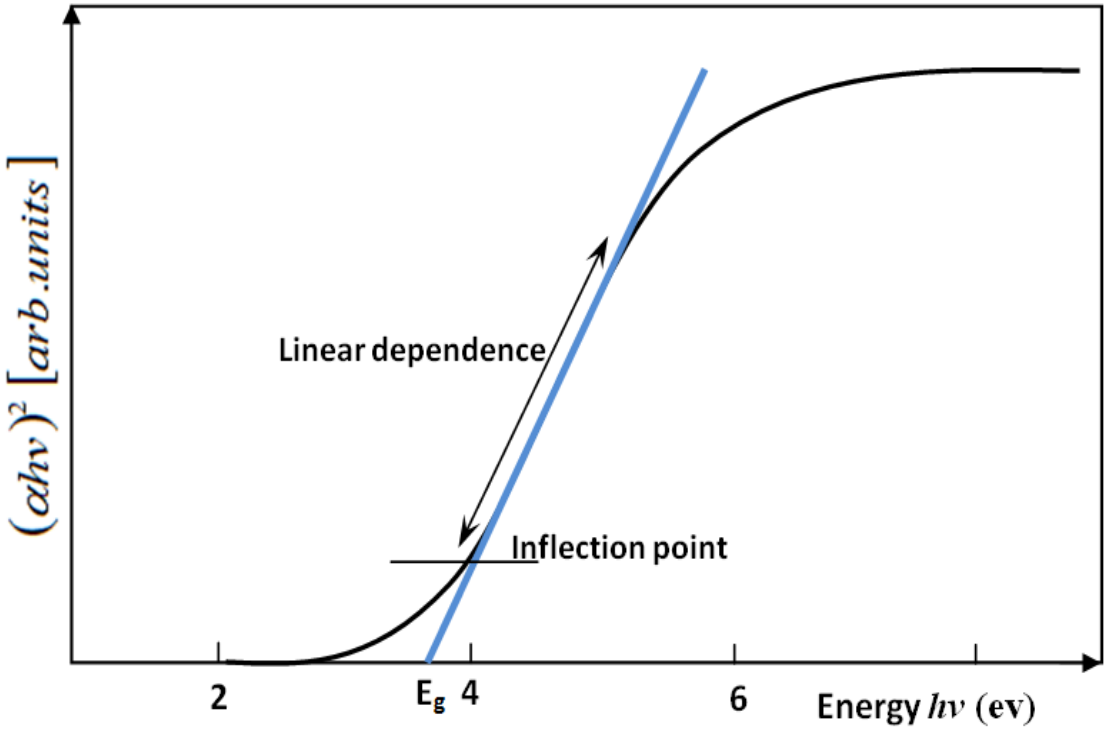

Figure II.18: Determination of the energy gap E_g by the extrapolation method from the variation of $(\alpha h\nu)^2$ as a function of hν for a thin layer. [91]

C. **Urbach energy:**

Mott and Dais noted that oppositely to pure crystalline structures, where the fundamental edge is mainly determined by conduction and valence levels, ion-doped binary semiconductor compounds present a particular optical absorption edge profile. In these materials, the absorption coefficient profile increases exponentially with the photon energy beneath the energy gap. This variation results in "blurring" of the valence conduction bands and narrows slightly the band gap by the occurrence of the so called Urbach tails (figure II.19).

Urbach tailing has been attributed, to various causes. Earliest investigations tried to relate it to the thermally induced lattice disorder [93, 94]. Generally, at optical absorption, near band edges, an electron from the top of the valence band gets excited to the bottom of the conduction band across the energy band gap. During this transition process, if these electrons encounter disorder, it causes changing in density of their states ζ (hν), tailing into the energy gap. This tail of ζ (hν) extending into the

energy band gap is termed as Urbach tail. Consequently, absorption coefficient α (hν) also tails off in an exponential manner and the energy associated with this tail is referred to as Urbach energy and can be calculated by the following equation [130].

$$\alpha = \alpha_0 \exp(\frac{h\nu}{E_u}) \quad \text{(II.20)}$$

$$\ln \alpha = \frac{1}{E_u}(h\nu) + \ln \alpha_0 \quad \text{(II.21)}$$

Where (α_0) is the pre-exponential factor, ($h\nu$) the photon energy and (E_u) is the band tail width commonly called Urbach energy. The band tail width is also related to the disorder in the film network [94, 95]. The Urbach energy, or the disorder, can be estimated from the inverse slope of the linear plot of ln (α) versus ($h\nu$) as represented in figure II.19.

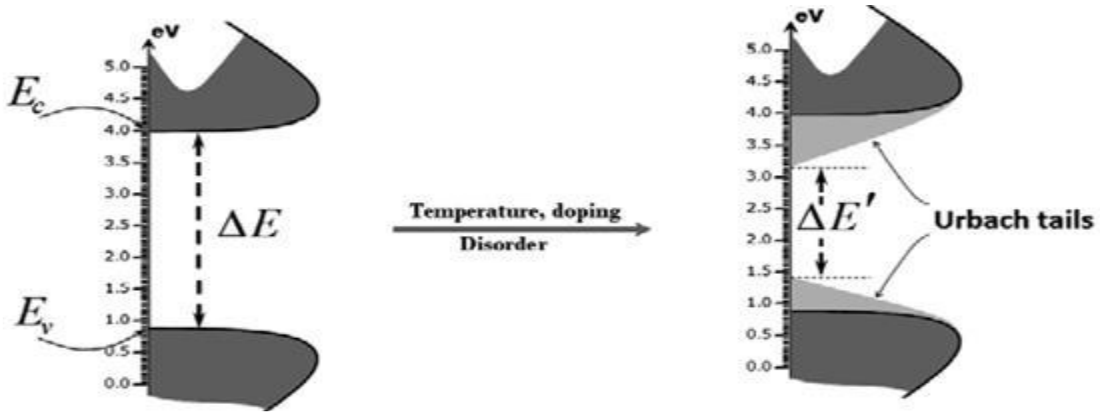

Figure II.19: Schema of Urbach tails [93].

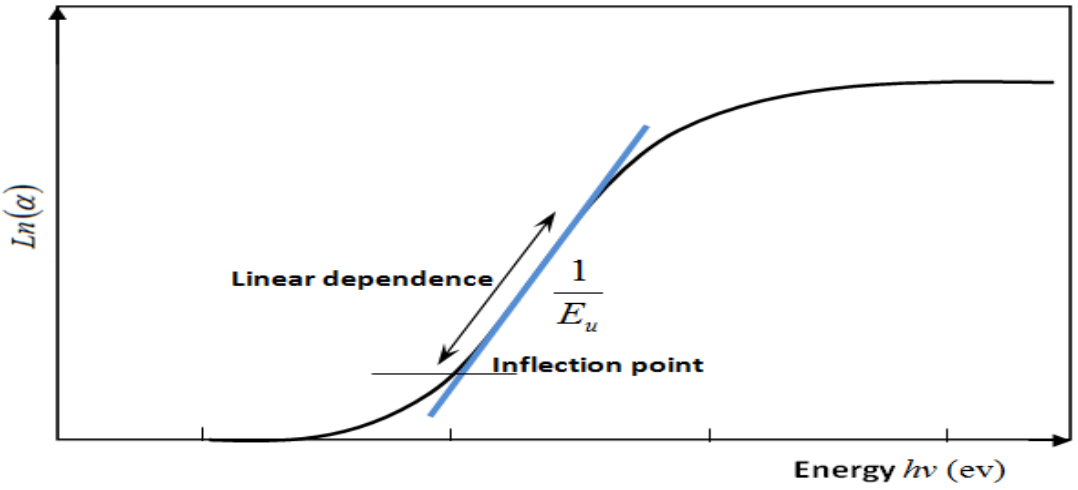

Figure II.20: determination of the Urbach energy from the variation of ln (α) as a function of $h\nu$ for a thin layer [95].

II.5.5.Method of four probes:

The four probes is commonly used technique to measure the semiconductor resistivity.

It is an absolute measurement without recourse to calibrated standards and is sometimes used to provide standards for other resistivity measurements. The schematic diagram of four probes measurement technique is shown in figure II.20. It is seen that by applying current (*I*) between outer probes in the figure II.21 and measuring voltage (*V*) between inner probes one can calculate the resistivity (ρ) and conductivity (σ) of the film using following equation [96].

$$\frac{1}{\sigma} = \rho = \frac{\pi}{\ln 2} t \frac{V}{I} = 4.5323 t \frac{V}{I} \qquad \text{(II.22)}$$

Where (*t*) is the film thickness.

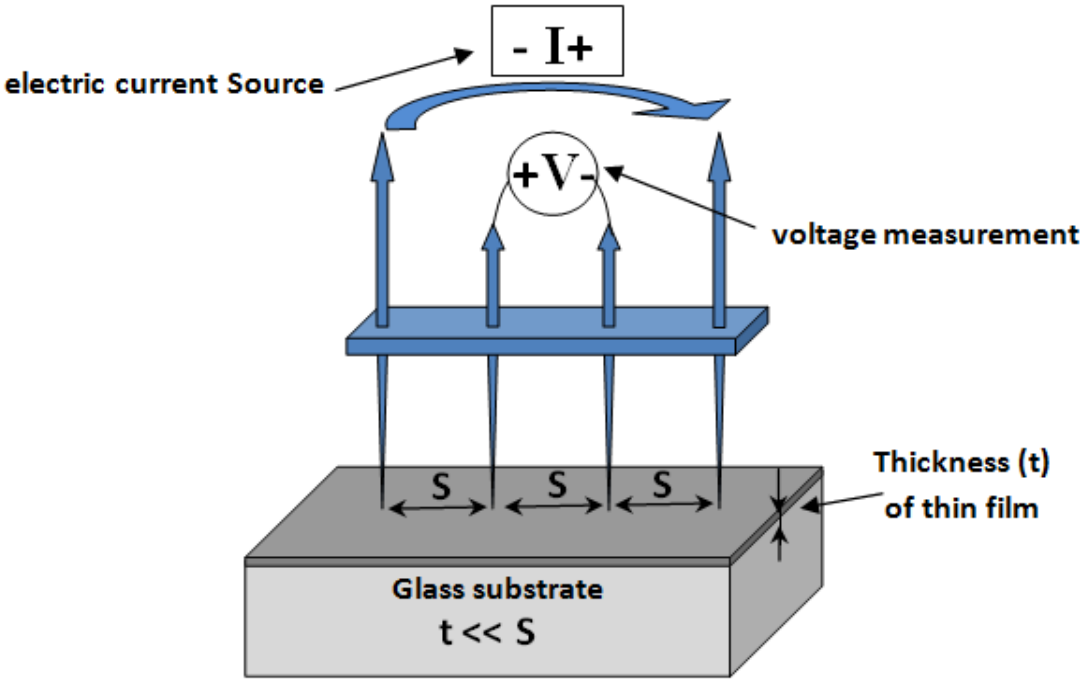

Figure II.21: Schematic diagram of four probes method [96].

II.6.Conclusion:

In this chapter, we have reported some of used preparation techniques for elaborating NiO thin films focusing on spray pyrolysis method that is the technique used in this work. Characterization tools also have been discussed for investigating the structural, morphological, optical analysis and electrical via X-ray diffraction, optical spectroscopy and four probes method.

Materials sciences and Engineering

CHAPTER 03: RESULTS AND DISCUSSION

III.1.Introduction

This chapter includes two parts; in the first part we describe the different steps of our experimental work in a detailed way. While in the second part, we present the results and the characterization techniques used in our work to measure the different properties (optical and electrical) than we discuss the obtained results.

III.2. Experimental Work:

III.2.1. Experimental conditions:

- ✓ The Substrate temperature: 400 °C.
- ✓ Spout-Substrate distance: 30 cm.
- ✓ The Quantity of the solution: 5 ml.
- ✓ The Deposit time: 15 - 20 min.
- ✓ Spray time: 8 – 12 sec
- ✓ Pressure: 2 bars.

II.2. 2.Experimental setups:

❖Calculate weights:

The weights were measured by sensitive electronic balance with four digits (10^4g) sensitivity figure III.1 .The appropriate weight of the materials $Ni(NO_3)_2.6H_2O$ were determined by using the following equation:

$$\mathbf{m = M \times C \times V} \qquad \text{(III.1)}$$

m: Mass Molar of the Powder (g).

M: Molar mass (mol).

C: The concentration (mol/L).

V: The volume of distilled water (L).

- **Calculate weight of $Ni(NO_3)_2.6H_2O$:**

Info:

- M_{Ni}= 58.693 g/mol, M_N= 14.01 g/mol, M_O= 16 g/mol and M_H= 1 g/mol.
- $M_{Ni\,(NO3)2.6H2O}$= 290.81 g/mol.
- C_1= 0.075 mol/L, C_2 = 0.10 mol/L, C_3=0.15 mol/L, C_4=0.20 mol/L.
- V = 0.1 L.

$\mathbf{m_1 = M \times C \times V}$

$= 290.81 \times 0.075 \times 0.1$

$m_{1\ Ni\ (NO3)2.6H2O} = 2.181075$ g

$\mathbf{m_2 = M \times C \times V}$

$= 290.81 \times 0.1 \times 0.1$

$m_{2\ Ni\ (NO3)2.6H2O} = 2.9081$ g

$\mathbf{m_3 = M \times C \times V}$

$= 290.81 \times 0.15 \times 0.1$

$m_{3\ Ni\ (NO3)2.6H2O} = 4.3621$ g

$\mathbf{m_4 = M \times C \times V}$

$= 290.81 \times 0.20 \times 0.1$

$m_{4\ Ni\ (NO3)2.6H2O} = 5.8162$g

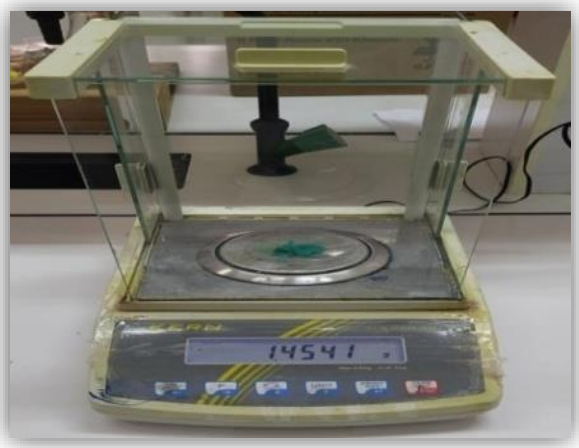

Figure III.1: Sensitive electronic balance at four digits (10^4g) sensitivity.

The different weight mass of the different molar concentration (0.075, 0.10, 0.15 and 020 M) are calculated and presented in the table III.1.

Table III.1: The weights of powder used in the preparation of the solution.

Molar concentration (M)	Weights (g)
0.075	$m_{1\ Ni\ (NO3)2.6H2O} = 2.1810$
0.10	$m_{2\ Ni\ (NO3)2.6H2O} = 2.9081$
0.15	$m_{3\ Ni\ (NO3)2.6H2O} = 4.3621$
0.20	$m_{4\ Ni\ (NO3)2.6H2O} = 5.8162$

III.2. 3.Preparation of solution:

- **$Ni(NO_3)_2.6H_2O$:** Green powder of Nickel Nitrate is the primary source of materials, with m1,m2,m3 and m4 dissolved in 100 ml of distilled water at 50 °C with different concentration of 0.075, 0.1, 0.15, 0.20 (mol/L).

Product Specification	
NICKEL (II) NITRATE (HEXAHYDRATE) AR	
PRODUCT CODE	593745
SYNONYMS	[Nickel (II) nitrate hexahydrate]
C.I. NO.	--
CASR NO.	(13478-00-7)
ATOMIC OR MOLECULAR FORMULA	$Ni(NO_3)_2.6H_2O$
ATOMIC OR MOLECULAR WEIGHT	290.79
PROPERTIES	Melting point 55°C
$Ni(NO_3)_2.6H_2O$	
PARAMETER	LIMIT
Description	Green crystals/crystalline powder.
Solubility	10% solution in water is bright and clear.
Minimum Assay (complexometric)	99.0%

Figure III.2: Profile of Ni $(NO_3)_2.6H_2O$ [97].

Figure III.3: Powder of Nickel Nitrate.

❖The solution preparation steps are as follows:

- ✓ Added to 100 ml of distilled water, the necessary amount of Nickel Nitrate for each concentration.
- ✓ Mixing everything with average speed of rotation using (Magnetic Stirrer) tray heated at temperature of 50 °C in 30 minutes to make sure that no residues were left and to ensure the homogeneity of the resultant solutions figure III.3.

- ✓ The resultant solution put it in glass bottle and kept to cool at the temperature of the room for 24 h figure III.5**.**

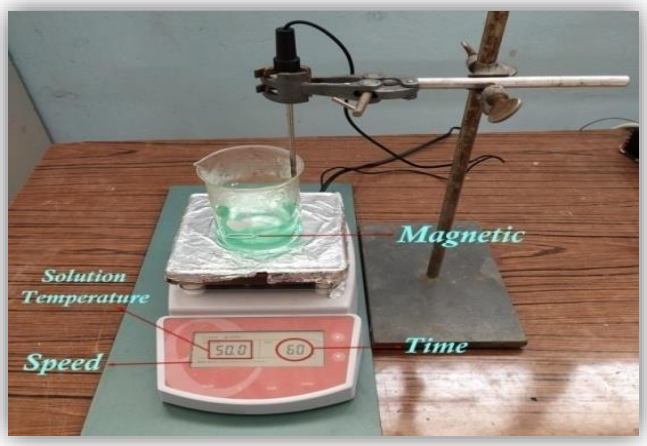

Figure III.4: (Magnetic stirrer) tray heated.

Figure III.5: Chemical Solution prepared.

This method of forming thin layers on glass substrates is done by the union.

The Nickel ions with the Oxygen ions present in the air of the furnace.

$$2\,(Ni\,(NO_3)_2.6H_2O) \xrightarrow[400\ ^\circ C]{} 2Ni \downarrow + 4NO_2 \uparrow + O_2 \uparrow + 12(H2O) \uparrow \qquad \text{(III.2)}$$

The Nickel ions are associated with Oxygen ions at a temperature of 400 °C. This solution is prepared with different weights of Nickel Oxide, as indicated in table III.1.

III.2. 4.Preparation of substrates:

A/Choice of substrate:

This choice allows us to carry out a good optical and electrical characterization of the layers; we used glass microscope slides with the dimensions of (25.4 x 76.2 mm²) and a thickness of 1-1.2 mm figure III.6.

The substrates used are glass slides; this choice of glass is due to three reasons:

- **1** It makes it possible to carry out a good optical characterization of the films which adapts well for their transparency.
- **2** After deposition, the sample (substrate + layer) will undergo a cooling from the deposition temperature above 400°C to ambient temperature (~ 25 °C) which causes compressibility of the two materials constituting the sample. In this case, they have very close expansion coefficients, which minimize the stresses. Note that an increase in the temperature of the substrate leads to an increase in stresses. This is linked to the compressive stress caused by the difference between the expansion coefficients of the substrate and of the material deposited :
  (α glass = 8.5×10^{-6} K^{-1}, α NiO = 7.93×10^{-6} K^{-1})
- **3** Economic reasons [98].

Figure III.6: Type of glass substrates used.

B/Cleaning of substrates:

The cleaning of the substrate is very important because it has a great effect on the properties of the films and the step determines the qualities of adhesion and homogeneity of the deposited layers, The quality of the deposit and consequently that of the sample depends on the cleanliness and the state of the substrate, remove all traces of grease and dust and visually check that the substrate surface is free of scratches and flatness clear as crystal. These conditions are essential for the good adhesion of the deposit to the substrate, and for its uniformity (constant thickness).to do this, it is essential to go through the substrate cleaning process because the electrical characteristics are very sensitive to surface preparation techniques.

- The process can be summarized by the following steps:

- Cleaning with (20 ml HCL + 100 ml distilled water) for 5 min at room temperature: « To remove any traces of grease and impurities attached to the surface of the substrate».
- Washing in a bi-distilled water bath for 5 min.
- Cleaning with (5 ml Methanol + 5 ml Acetone) for 5 min:

«This reacts with contamination such as grease and some oxides».

- Washing in a bi-distilled water bath.
- And finally, drying using an electrical oven and Josef paper.

❖ Avoid touching the surface of the substrate to avoid contamination.

C/Cuts & remarks of substrates:

The figure III.7 show the methods of cuts and the devising of the substrates to 3 section of (2.5× 2.5) Cm².

Figure III.7: The substrates cuts.

II.2.5.System of chemical spray pyrolysis:

Figure III.8-9 show the chemical spray pyrolysis system used in the preset work.

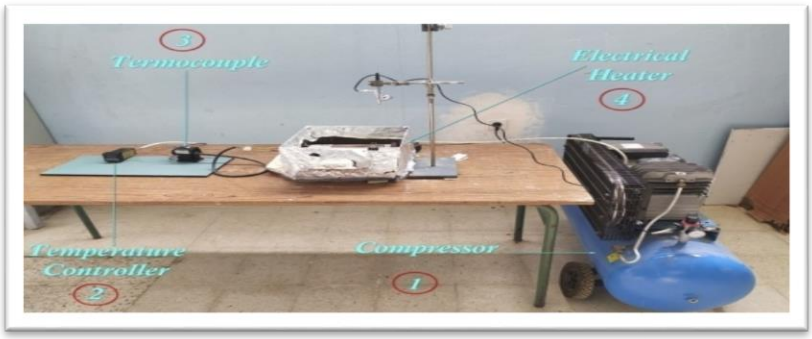

Figure III.8: Experimental setups of the homemade pyrolysis spray system.

Figure III.9: Experimental homemade device of the pyrolysis spray technique.

- The main elements of this assembly are :

1. Air compressor:

Under a controllable pressure (P = 2 bar) the compressor pushes the pressurized air drop from glass bottle; this leads to make the solution flows from the capillary tube to the glass substrates, as soft spray.

2. Thermocouple:

This includes a sensitive thermal wire; it is attached to the hot plate and joined to the digital temperature controller which fixes the temperature of the surface of the plate to the desired value.

3. Temperature controller: this is the device related to thermocouple and to the sensitive heat detector on the electrical heater which gives the choice of temperature degree (400°C).

4. Electrical heater:

The heater is used for heating the plate on which the glass substrate is placed, to deposit the thin film. In this study the temperature used was 400± 20 ° C.

5. Airbrush:

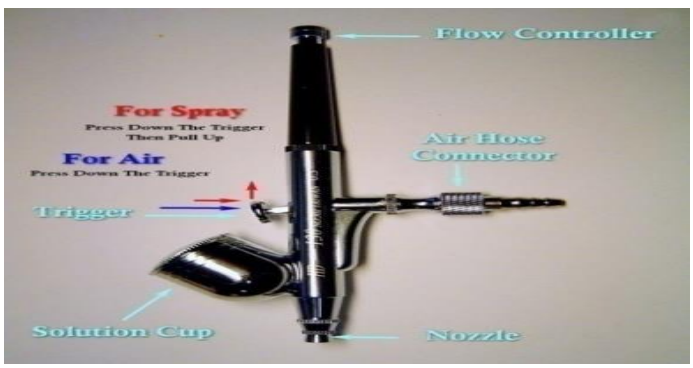

Figure III.10: Royal_Max Airbrush Gun.

III.2.6.Parameters affects the films deposition [99]:

a) Atomizing Air Pressure:

The air pressure was kept at (2 bar) to get uniform films the air pressure inside nozzle was adjusted to obtain fine atomizes in order to avoid the rapid decrease in substrate temperature which will cause the glass substrate to be broken.

b) Substrate temperature:

One of the important parameters is substrate temperature it significant affect the homogeneity of the prepared films, because it is responsible for the variation of the crystal structure of the material that affects the physical properties of the materials.

c) Spraying rate:

Sprayer rate might cause a significant decrease in substrate temperature and lead to substrate crush. This parameter affects the homogeneity and thickness of the prepared films. In this study the spraying rate of the films was kept at (1.5 – 2 ml/min) to ensure a good stoichiometry and obtain a homogenous film.

d) Spraying time:

It is important to control the time period between every spraying operation, it should be uniform, and the spraying time period was 8-12 sec with 3- 3.5 minutes wait between any two successive sprayings.

e) Nozzle to Substrate Distance :

To obtain uniform film it's important to check the distance from the end of the capillary tube to the substrate. In the present experiment the distance was fixed at 30cm.

Different distance causes scattering of the atomized solution away from the substrate, also any decrease in this distance will cause the collection of solution drops in one spot and this will affect film homogeneity.

III.3.Result and discussion:

This part includes the description and the analysis of the measurements and the discussion of the results. It focuses on optical properties of Nickel oxide (NiO) with different molarities (0.075, 0.10, 0.15 and 0.20 M).

Figure III.11 shows the photo images of Nickel oxide (NiO) thin films, with different molarities (0.075, 0.10, 0.15 and 0.2 M). It is reported that the stoichiometry correct NiO thin films are expected to have green color [11-12]; however, the NiO thin films deposited in the present study have black-grey color which can be explained by the non-stoichiometry of the deposited material.

0.075M 0.10M 0.15M 0.20M

Figure III.11: photo images of Nickel oxide (NiO) thin films.

III.3.1.Optical analysis:

The optical measurement results include relations of the transmittance and absorbance with wavelength for Nickel oxide (NiO) thin films with different molarities (0.05, 0.1, 0.15 and 0.2 M) and computing some optical parameters like absorption coefficient, Transmittance coefficient, optical energy gap and Urbach energy.

Optical absorption spectra of the films in spectral range of (300-1100 nm) were recorded by using UV–Vis spectrophotometer.

The analysis of the dependence of absorption coefficient on photon energy in the high absorption regions is performed to obtain the detailed information about the energy band gap of the films.

III.3.1.1 Transmittance:

Figure III.12 shows the relation between transmittance and wavelength for NiO thin films at different molarities. It is clear that the transmittance for all samples increases rapidly as the wavelength increases in the range of (300- 350 nm), and then increases slowly at higher wavelengths. The spectra show high transmittance in the visible and infrared regions, and low in the ultraviolet region. It can be noticed also that the fundamental absorption edge is sharp in the visible region of the spectrum. The

transmittance increases with increase in the molarity of the solution and the molarity 0.2M has a maximum transmittance of nearly equal to 65%.

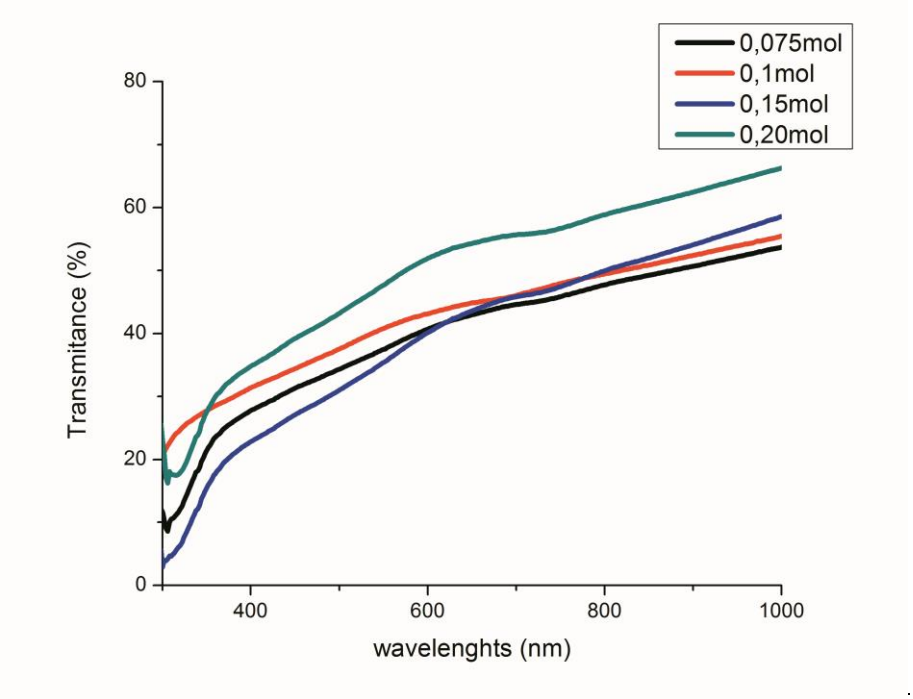

Figure III.12: Transmittance (T) versus wavelength (λ) of Nickel oxide thin films at different molarities.

III.3.1.2 Absorption:

The variation of the absorbance spectrum with wavelength is opposite to the transmittance spectrum. The study of absorbance was in the range of (300– 1100 nm). Figure III.13 shows the relation between absorbance (A) and wavelength for NiO Nickel oxide thin films. The absorbance decreases rapidly at short wavelengths (high energies) corresponding to the energy gap of the film, (when the incident photon has an energy equal or more than the energy gap value). This evident increase of energy is due to the interaction of the material electrons with the incident photons which have enough energy for the occurrence of electron transitions, this attribute to decrease the energy gap of the film.

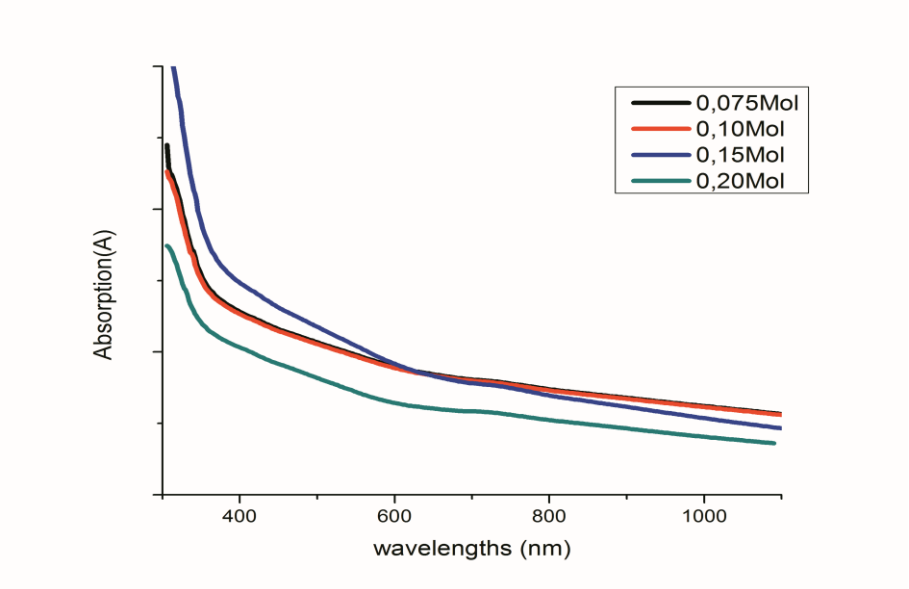

Figure III.13: Absorbance (A) versus wavelength (λ) of Nickel oxide thin films of different molarities.

We can calculate the absorption coefficient using equation (II.16):

$$\alpha = (2.303 \times A)/t \qquad \text{(III.3)}$$

Where A is the absorbance**,** t=300nm is the thickness and (α) is the absorption coefficient. It have been noticed that all the prepared thin films have high absorption coefficient in visible range of the spectrum, and this could be seen in figure (III.14) which shows the relation between the absorption coefficient (α) with photon energy (hυ) of Nickel oxide thin films. The absorption coefficient increases with increase in photon energy (hυ). The absorption coefficient value depends on absorbance.

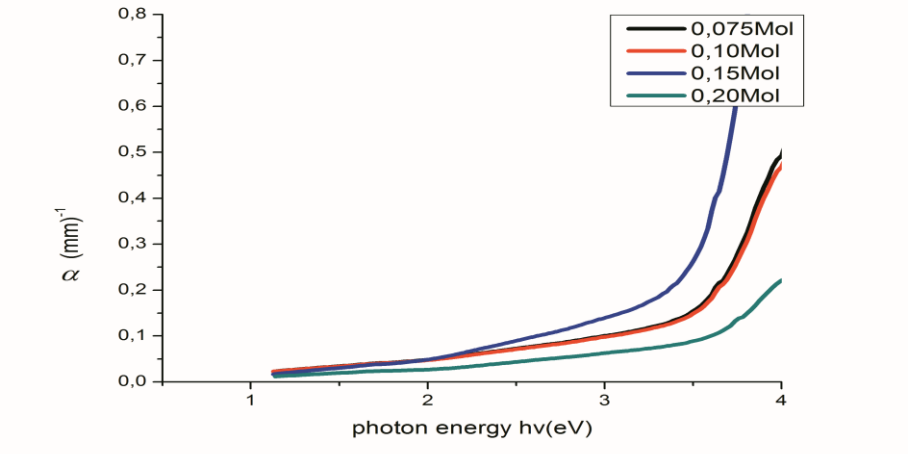

Figure III.14: The relation between absorption coefficient and photon energy of Nickel oxide thin films at different molarities.

III.3.1.3 Optical Energy gap (Eg):

The energy gap values depend in general on the films crystal structure, the arrangement and distribution of atoms in the crystal lattice, also affected by crystal regularity. The optical energy gap (Eg) was derived assuming allowed direct transitions between the edge of the valence and conduction band.

The energy gap was calculated using equation (II.19), by plotting a graph between $(\alpha h\nu)^2$ and $(h\nu)$ in eV, a straight line is obtained which gives the value of the direct band gap. The extrapolation of the straight line to $(\alpha h\nu)^2 = 0$ gives value of the direct band gap of the material, and this could be seen in figure III.15.

Once notice that the band gap value decreases when the molarity increases, which is in agreement with other reports. This decrease in the band gap can be related to the structural modification of the films with higher molarity.

However, many reports reported that the change in the optical band gap energy with molarity may be attributed to the changes in homogeneity and crystallinity of the film, caused by difference in experimental conditions, mainly the amount of spraying solution, spray rate and cooling of the substrates during deposition .The allowed direct band gap values range between 3.068eV to 3.480 eV for the prepared samples, as shown in table (III.2). Figure (III.15) represents the variation of energy gap as a function of molarity for all the deposited thin films in this study.

Table III.2: Energy gap of Nickel oxide thin films at different molarities.

Molarity (M)	Gap energy Eg (eV)
0.075	3.360
0.10	3.068
0.15	3.480
0.20	3.369

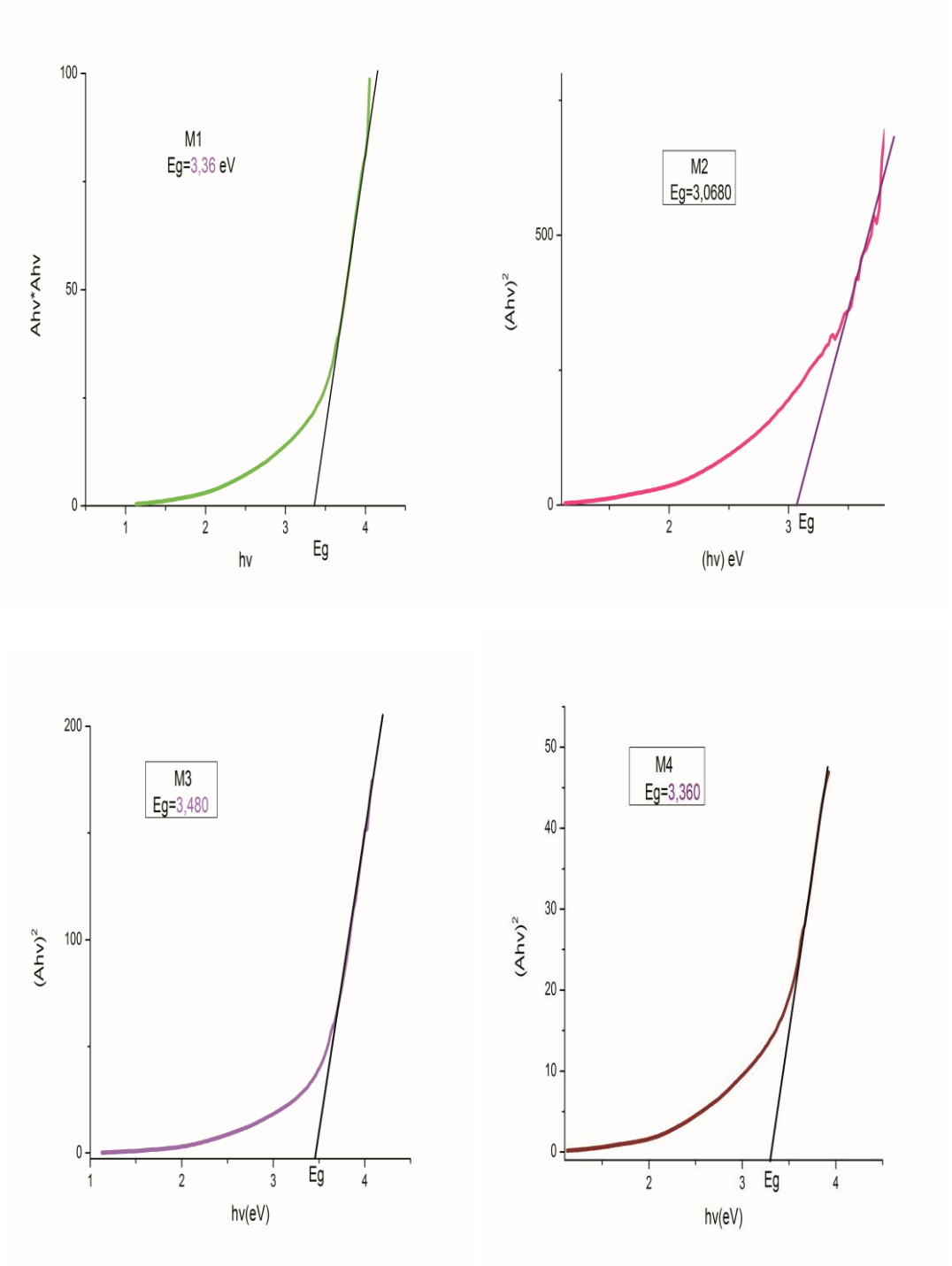

Figure III.15: The relation between $(h\upsilon)^2$ and $(h\upsilon)$ of Nickel oxide thin films at different molarities.

III.3.1.4 Urbach Energies (Eu):

The Urbach energy can be calculated using equation (II-21). Figure (III-16), shows Urbach plots of the undoped NiO thin films. The values of (Eu) were obtained from the inverse of the slope of (ln A) versus $(h\upsilon)$.

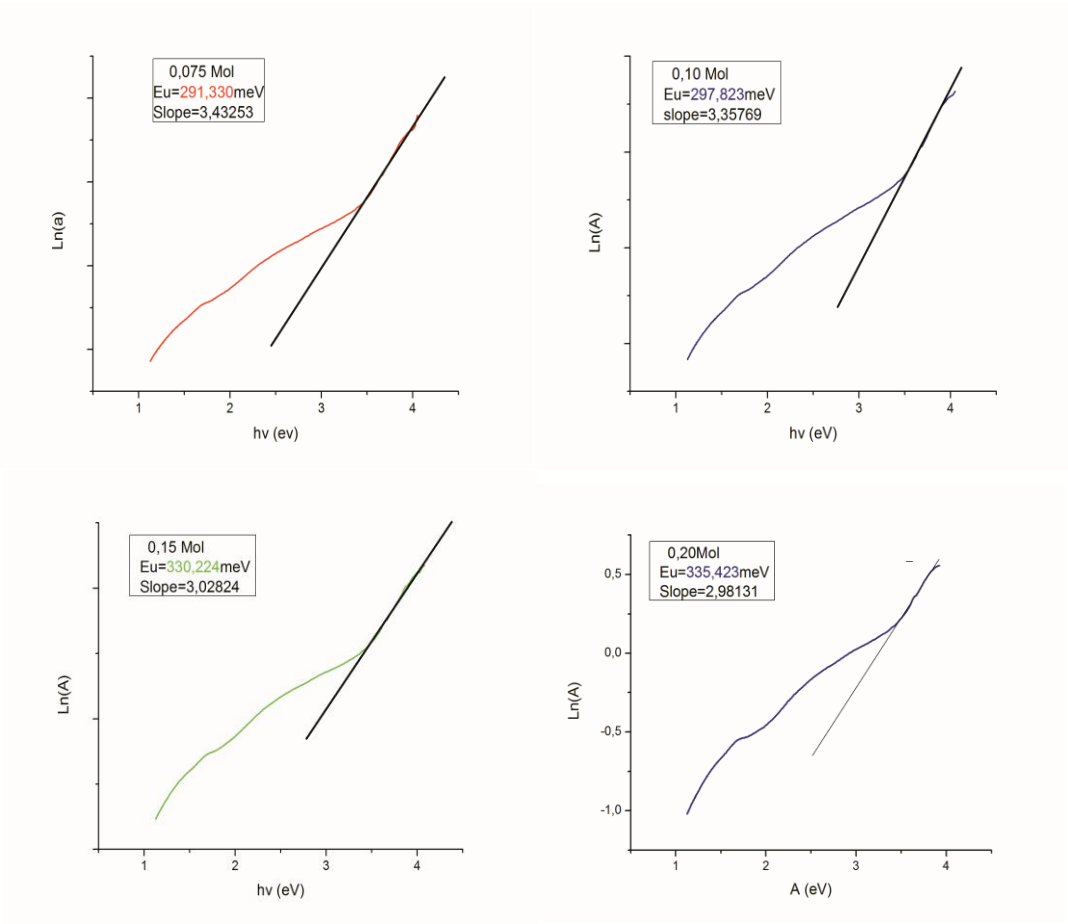

Figure III.16: The Urbach plots of NiO thin films at different molarities.

It is observed that the Urbach energy increases as the molarity increasing. As shown in figure III.17

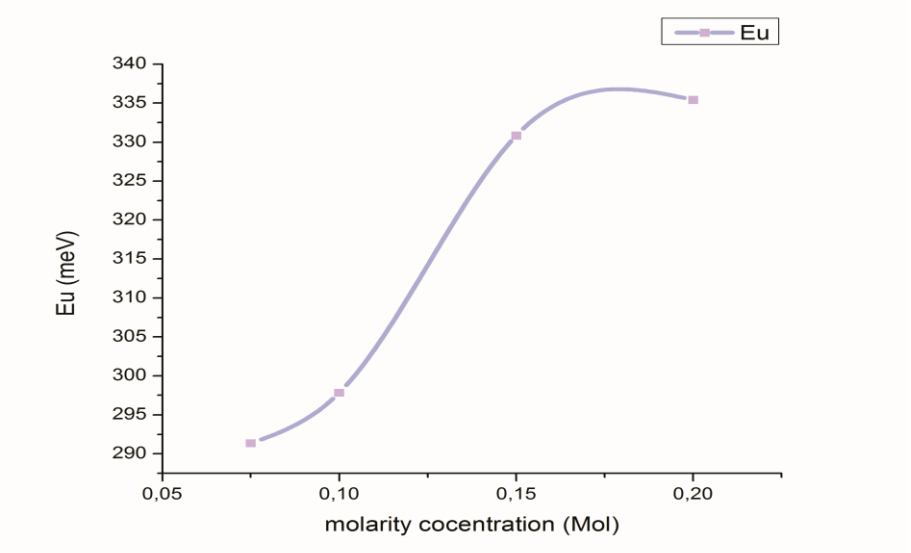

Figure III.17: The variation of Urbach energy as a function of molarity for Nickel oxide thin films.

Table III.3: Urbach energy of Nickel oxide thin films at different molarities.

Molarity (M)	Urbach energy Eu (meV)
0.075	291.330
0.10	297.823
0.15	330.224
0.20	335.423

III.3.1.5.Extinction Coefficient (K_o):

The extinction coefficient (K_o) was calculated using relation (II.18). The study of extinction coefficient (K_o) was in the range of (300 - 1100) nm.

Figure III.18 shows the extinction coefficient as a function of wavelength for Nickel oxide thin films.

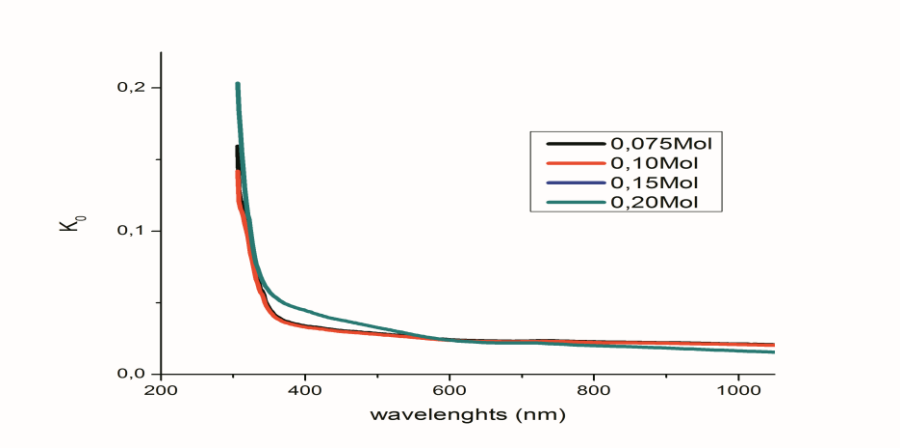

Figure III.18: The relation between the extinction coefficient K_0 and wavelength for Nickel oxide thin films at different molarities.

The extinction coefficient (K_o) decreases rapidly at short wavelengths (300-400) nm and after that the value of (K_o) remains constant. The rise and fall in the value of (K_o) is directly related to the absorption of light. The lower value of (K_o) in the wavelength range (400–1100) nm implies that these films absorb light in this region very easily. The change in extinction coefficient with the solution molarity was not systematic.

III.3.1.6.Relation between Eg and Eu:

Figure III.19.Shows the variation of the optical Gap and Urbach energy of NiO thin films versus molarity concentration.

We have noticed that most Urbach energy values varied inversely proportional with the most energy band gaps values versus molarity concentration in the solution of films.

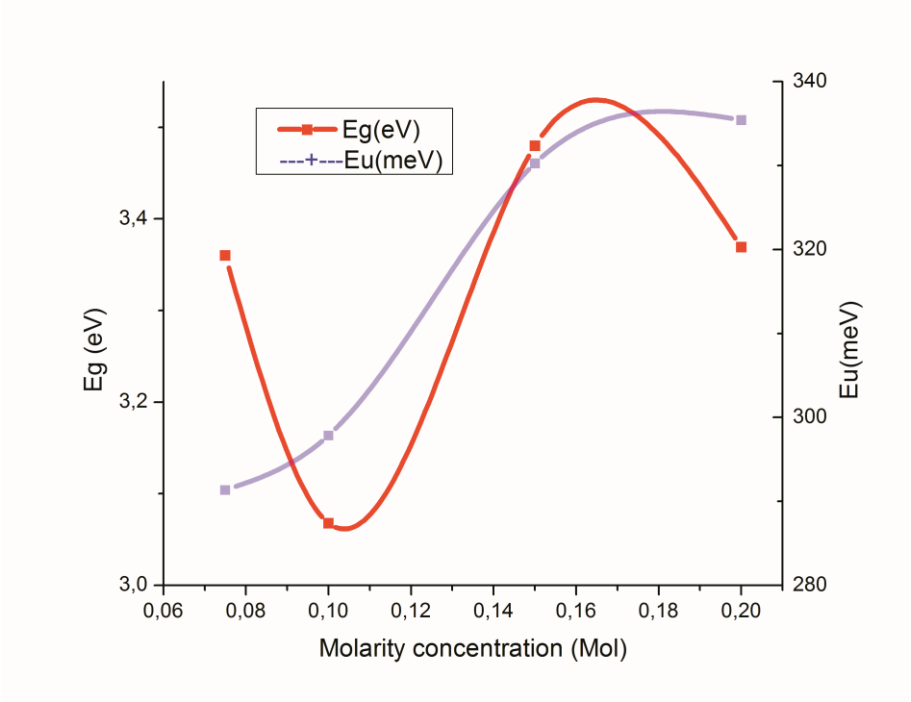

Figure III.19: Variation of the optical Gap and Urbach energy of NiO thin films versus Molarity concentration.

III.4.Conclusion:

In this study Nickel oxide thin films, were successfully deposited on glass substrate at (400 ºC) with different molarities by chemical spray pyrolysis technique.

The average optical transmittance for NiO is above 40 % in the visible region, where as the optical band gap value change from 3.480 to 3.068 eV as molarity concentration increases.

The Urbach energy increases as the molarity concentration increases and the Urbach energy values range between 291.330 meV and 335.423 meV.

Materials sciences and Engineering

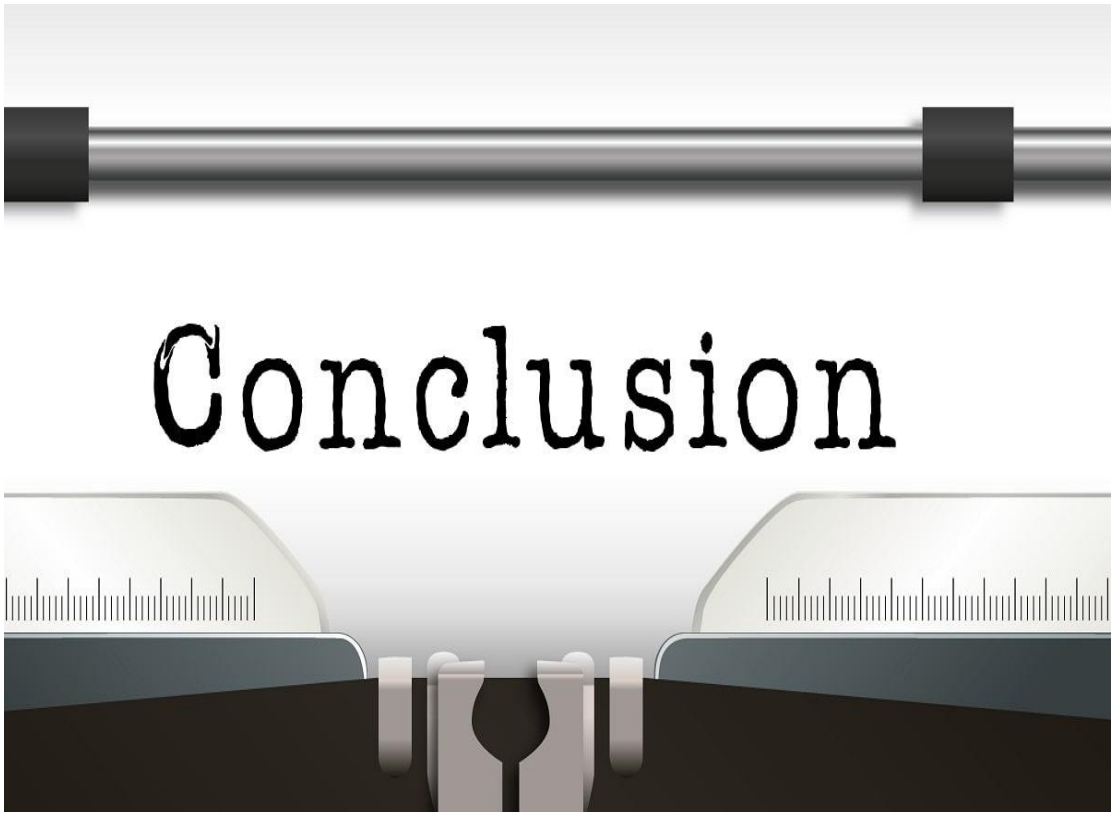

GENERAL CONCLUSION

General conclusion:

The main goal of this thesis is the preparation and characterization of thin films based on Nickel oxide (NiO) with different solution molarities. This work is started with the preparation of samples using a very low coast homemade is the chemical spray pyrolysis technique.

In this study Nickel oxide films were successfully deposited by spray pyrolysis technique on glass substrates at temperatures above 400 °C and a very well chosen parameters with different solution molarities (0.075, 0.10, 0.15 and 0.20M) then the samples were investigated using UV-visible spectrophotometer.

The NiO thin films deposited in the present study have black-grey color which can be attributed to the non-stoichiometry of the deposited material.

The aim of this work is to study the effect of different molarity solution of Nickel Oxide on the structural, optical and electrical properties. To characterize these samples, we have to use several techniques, such as X-ray diffraction for structural characterization, UV-Visible spectroscopy for optical characterization, the four-point method for electrical characterization and weight difference methods for thickness measurement. Unfortunately the sanitary situation on the country for this school year doesn't allow the practice of any techniques out of our university which the only possible one was at our university is the UV-Visible spectroscopy for the optical characterization what gives some results as followed:

The transmission and absorption spectra of the sprayed NiO thin films in the wavelength range of 300-1100 nm. As the transmittance of Nickel Oxide thin films increases rapidly as the wavelength increases in the range of (300-400) nm, and then increases slowly at higher wavelengths.

It is observed that the transmission is about 22-65 % in the visible range and it increases to the maximum which is 65 % in the infrared domain for the molarity concentration of 0.20 M.

Whereas the optical band gap value change from 3.480 to 3.068 eV as Molarity concentration increases.

The Urbach energy increases as the molarity concentration increases and the Urbach energy values range between 291.330 meV and 335.423 meV.

At the end we noticed that the best molarity concentration for Nickel Oxide is 0.20 M, where was the best transmittance = 65%, Gap energy = 3.369 eV and Urbach energy= 335.423 meV.

Future Works:

According to the results of this study, the following future studies are suggested:

1. Studying the electrical properties for Nickel oxide thin films at different molarities.
2. Studying the structural properties for Nickel oxide thin films at different molarities by X-ray diffraction.
3. Studying the structural properties (Surface morphological studies) of Nickel oxide thin films by Scanning Electron Microscopic.
4. Preparation of Nickel oxide thin films by another technique like thermal evaporation technique or sol-gel technique.

Abstract:

In this work, NiO thin films at different molarities (0.05, 0.1, 0.15 and 0.2M) have been successfully deposited on glass substrates by chemical spray pyrolysis (CSP) technique at substrate temperature of (400^{o}C) .The optical properties of these films have been investigated using UV-Visible spectroscopy. The absorbance and transmittance spectra have been recorded in the wavelength range of (300-1100) nm in order to study the optical properties .The optical energy gap for allowed direct electronic transition was calculated using Tauc equation. It is found that the band gap changes when the molarity increases and the band gap values range between 3.068 eV and 3.480 eV for the prepared NiO thin films at different molarities. The Urbach energy increases as the molarity increases and the Urbach energy values range between 291.330 meV and 335.423 meV. The optical constant absorption coefficient was also calculated as a function of photon energy. Extinction coefficient for NiO thin films were estimated as a function of wavelength.

Key words: NiO thin films, Solution Molarity, Chemical Spray Pyrolysis, Optical Properties.

ملخص:

في هذا العمل، تم ترسيب أغشية NiO الرقيقة في مولات مختلفة (0.05 ، 0.1، 0.15 و 0.2M) بنجاح على ركائز زجاجية بتقنية الانحلال الحراري بالرش الكيميائي (CSP) عند درجة حرارة الركيزة (400 درجة مئوية). تم فحص هذه الأفلام باستخدام التحليل الطيفي للأشعة فوق البنفسجية المرئية. تم تسجيل أطياف الامتصاص والنفاذية بمدى أطوال موجية (300-1100) نانومتر لدراسة الخواص الضوئية ، وتم حساب فجوة الطاقة الضوئية للانتقال الإلكتروني المباشر المسموح به باستخدام معادلة Tauc. لقد وجد أن فجوة النطاق تتغير عندما تزداد المولية وتتراوح قيم فجوة النطاق بين 3.068 فولت و 3.480 فولت لأغشية NiO الرقيقة المحضرة عند مولات مختلفة. تزداد طاقة Urbach مع زيادة المولية وتتراوح قيم طاقة Urbach بين 291.330 meV و 335.423 meV. تم حساب معامل الامتصاص البصري الثابت أيضًا كدالة لطاقة الفوتون. تم تقدير معامل الاندثار الجزيئي الغرامي لأغشية NiO الرقيقة كدالة لطول الموجة.

الكلمات المفتاحية: أغشية NiO الرقيقة ، مولية المحلول ، التحلل الحراري بالرش الكيميائي ، الخواص البصرية.

Résumé :

Dans ce travail, des couches minces de NiO à différentes molarités (0,05, 0,1, 0,15 et 0,2 M) ont été déposés avec succès sur des substrats en verre par la technique de pyrolyse par pulvérisation chimique (CSP) à une température de substrat de (400 ° C).Ces films ont été étudiés par spectroscopie UV-visible. Les spectres d'absorbance et de transmittance ont été enregistrés dans la gamme de longueurs d'onde de (300-1100) nm afin d'étudier les propriétés optiques. L'écart d'énergie optique pour la transition électronique directe autorisée a été calculé en utilisant l'équation de Tauc. On constate que la bande interdite change lorsque la molarité augmente et que les valeurs de bande interdite se situent entre 3,068 eV et 3,480 eV pour les films minces de NiO préparés à différentes molarités. L'énergie d'Urbach augmente à mesure que la molarité augmente et les valeurs d'énergie d'Urbach varient entre 291,330 meV et 335,423 meV. Le coefficient d'absorption optique constante a également été calculé en fonction de l'énergie photonique. Le coefficient d'extinction des couches minces de NiO a été estimé en fonction de la longueur d'onde.

Mots clés: Couches minces de NiO, molarité de la solution, pyrolyse par pulvérisation chimique, propriétés optiques.

REFERENCES:

[1] S. Yahiaoui, "L'effet de la molarité des différentes sources d'étain sur les propriétés des couches minces d'oxyde d'étain SnO2 élaborées par Spray Ultrasonique", Magister Thesis, Biskra University, Algeria, (2014).

[2] D. Royer and E. Dieulesaint, "Ondes élastiques dans les solides (Génération, interaction acousto-optique, applications)", Edition Masson, Tome 2, France (1999).

[3] M. Boussafeur, "Elaboration par ‹‹ spray pyrolyse ›› et caractérisations structurales de couches minces d'oxyde de zinc" Master thesis, Larbi Ben M Hidi University Oum El-Bouaghi, Algeria, (2012).

[4] J. Aronovich, A. Ortiz and R. H. Bube, J.Vac.Sci. Technol. 16.994 (1979).

[5] J. F. Chang, C. C. Shen and M. H. Hon, Ceramics Internet 29 (2003).

[6] http://fr.wikipedia.org/wiki/couche_mince.57.

[7] https://www.cefi.org (Fra DESS.old / dess_265 html).

[8] S. Yamaga, A. Yoshokawa, H. Kasain, Cryst. Growth 86 (1998).

[9] I.C. Ndukwe, Sol. Energy Mater. Ground, Cells 40 (1996).

[10] T.E. Varitimos, R.W. Tustison, thin Solid Films 151 (1987).

[11] Benoit Chavillon, thèse de doctorat, Synthèse et caractérisation d'oxydes transparents conducteurs de type p pour application en cellules solaires à colorant matériaux. Université de Nantes, France, (2011).

[12] Greenwood, Norman N, Earnshaw, Alan, «Chemistry of the Elements", Oxford, Pergamon Press, (1984)

[13] Z. Zhiwei, Oxygen reduction on lithium nickel oxide as a catalyst and catalyst support, PhD thesis, Case Western Reserve University, (1993).

[14] A. M. Soleimanpour, Synthesis, fabrication and surface modification of monocrystalline nickel oxide for electronic gas sensors, PhD thesis, University of Toledo, (2013).

[15] M. Krunks, J. Soon, T. Unt, A. Mere, and V. Mikli, "Deposition of p-type NiO films by chemical spray pyrolysis," Vacuum, vol. 107, pp. 242–246, (2014).

[16] N. Banerjee and K. K. Chattopadhyay, "Recent developments in the emerging field of crystalline p-type transparent conducting oxide thin films," Prog. Cryst. Growth Ch., vol. 50, pp.52-105, (2005).

[17] I. Sta, M. Jlassi, M. Hajji, and H. Ezzaouia, “Structural , optical and electrical properties of undoped and Li-doped NiO thin films prepared by sol-gel spin coating method,” Thin Solid Films, vol. 555, pp. 131–137, (2014).

[18] S. Kerli, U. Alver, and H. Yaykas, “Applied Surface Science Investigation of the properties of in doped NiO films,” Appl Surf Sci, vol. 318, pp. 164–167, (2014).

[19] M. Jlassi, I. Sta, M. Hajji, and H. Ezzaouia, “Optical and electrical properties of nickel oxide thin films synthesized by sol-gel spin coating,” Mater. Sci. Semicond. Process., vol. 21, no. 1, pp. 7–13, (2014).

[20] Y. R. Park, K. J. Kim, Sol-gel preparation and optical characterization of NiO and Ni1-xZnxO thin films,” J. Cryst. Growth, vol. 258, pp. 380–384, (2003).

[21] W. Nolting, L. Haunert, G. Borstel, “Temperature-dependent electronic structure and magnetic behavior of Mott insulators,” Phys. Rev. B, vol. 46, pp. 4426–4445, (1992).

[22] O. Bengone, M. Alouani, P. Bl. Ochl, J. Hugel, “Implementation of the projector augmented-wave LDA+U method: Application to the electronic structure of NiO,” Phys. Review B, vol. 62, pp. 16392–16401, (2000).

[23] A. J. Hassan, Study of Optical and Electrical Properties of nickel oxide (NiO) Thin Films Deposited by Using a Spray Pyrolysis Technique, Journal of Modern Physics, 518 (2014).

[24] N. Tsuda, K. Nasu, A. Fujimori, K. Siratori, Electronic Conduction in Oxides, second ed., Springer, Berlin, (2000).

[25] P. Pramanik, S. Bhattachraya, a Chemical Method for the Deposition of nickel oxide Thin Films, J. Electrochemical. Soc., 137 (1990).

[26] R.S. Conell, D.A. Corrigan, B.R. Powell, The electro chromic properties of sputtered nickel oxide films, Solar Energy Mater Solar Cells, (25) 301-313 (1992).

[27] R. J. Powell, W. E. Spicer, Optical Properties of NiO and COO, (Physical Review B Solid State), 2 (1970).

[28] H.A.E. Hagelin-Weaver, J.F. Weaver, G.B. Hoflund, G.N. Salaita, Electron energy loss Spectroscopic investigation of Ni metal and NiO before and after surface reduction by Ar+ bombardment, Journal of Electron Spectroscopy and Related Phenomena, 134 (2004).

[29] K.S. Lee, H.J. Koo, K.H. Ham, W.S. Ahn, Crystal Molecular Orbital Calculation of The Lanthanum nickel oxide by Means of the Micro Soft Fortran, Bull. Korean. Chem, Soc., 16 (1995).

[30] S. Hüfner, T.riserer, Electronic structure of NiO, Physical Review B, 33 (1986).
[31] A.R. Williams, J. Kübler, K. Terakura, Phys. Rev. Lett, 54 (1985).

[32] A. Noua, Doctorate LMD thesis, Larbi Ben M Hidi University Oum El-Bouaghi, (2019).
[33] Francisco Anderson de Sousa Lima, Doctorate thesis , Application of transition metal- oxide-based nanostructured thin films on third generation solar cells, Universidade Federal do Ceará , (2015).
[34] Bhachu D, Doctorate thesis, The synthesis and characterization of metal oxide thin films. University College London, (2013).
[35] Fellahi OU, thèse de doctorat, Élaboration de nano fils de silicium par gravure chimique assistée par un métal: caractérisation et application en photocatalyse hétérogène de l'oxyde de graphène, du chrome (VI) et de la rhodamine B, Université Sétif 1, Algérie, (2014).
[36] Sze, Simon M., and Kwok K. Ng. Physics of semiconductor devices. John wiley & sons, (2006).
[37] Lahcène D, thèse de doctorat, étude d'un système autonome pour le traitement des eaux usées par les techniques membranaires .membranes a effet photocatalytique a base de TiO2, Université Hassiba Ben Bouali Chlef, Algérie, (2011).
[38] Tamez Uddin Md., Doctorate thesis, Metal Oxide Hetero structures for Efficient Photocatalysts, Technical University of Darmstadt- Germany, (2013).
[39] Fujishima, Akira, and Kenichi Honda. "Electrochemical photolysis of water at a semiconductor electrode." Nature, vol. 238. 5358, pp. 37, (1972).
[40] Robert Waugh M, Doctorate thesis, The Synthesis, Characterization and Application of Transparent Conducting Thin Films, University College London, (2011).
[41] Saâd Rahmane, thèse de Doctorat, Elaboration et caractérisation de couches minces par spray pyrolyse et pulvérisation magnétron, Université Mohamed Kheider– Biskra, Algérie, (2008).
[42] https://www.researchgate.net/figure/10-Cathodic-sputtering-accelerated-Ar-ions-extract atoms-from-the-target_fig9_278637056 [accessed 16 May, 2020].
[43] Khachab Hamid, thèse de Doctorat, Modélisation de la croissance épitaxiale par jets moléculaires (MBE) avec la méthode de Monte Carlo Cinétique (KMC), Université Abou-Bekr Belkaid -Tlemcen, Algérie, (2010).

[44] Gabriel Tourbot, thèse de Doctorat, Croissance par épitaxie par jets moléculaires et détermination des propriétés structurales et optiques de nano fils InGaN/GaN, Université de Grenoble, France, (2012).

[45] Esteban Martinez-Guerrero, thèse de Doctorat, Elaboration en Epitaxie par Jets Moléculaires des Nitrures d'éléments III en Phase Cubique, Institut National des Sciences Appliquées de Lyon, France, (2002).

[46] Taabouche Adel, thèse de Doctorat, Etude structurale et optique de films minces ZnO Elaborés par voie physique et/ou chimique, Université Frères Mentouri Constantine I, Algérie, (2015).

[47] K.C. Sanal, Development of p-type transparent semiconducting oxides for thin film transistor applications, PhD thesis, cochin university of science and technology, (2014).

[48] K. Badeker, Annalen der Physik 327, 749-66.

[49] C.M. Wang, C.Y. Wen, Y.C. Chen, K.S. Kao, D.L. Cheng, C.H. Peng, Effect of deposition temperature on the electro chromic properties of electron beam-evaporated WO3 thin films, Integrated Ferroelectrics, 158 (2014) 62-68.

[50] Kefif Kheira, thèse de Doctorat, Elaboration et caractérisation optique des Semi-conducteurs amorphes et nanocristallins de silicium (a-Si :H, nc-Si :H) et de carbure de silicium (a-SiC :H, nc-SiC :H), Université d'Oran 1, Algérie, (2015).

[51] Maria Magdalena Şovar, thèse de Doctorat, du tri-iso propoxyde aux oxydes d'aluminium par dépôt chimique en phase vapeur : procédé, composition et propriétés des revêtements obtenus, INP Toulouse et Université Polytechnique de Bucarest, Romania (2006).

[52] Bachelet, Romain, thèse de Doctorat, Couches minces d'oxydes élaborées par voie Sol-gel, épitaxies et nanostructures par traitements thermiques post-dépôt, Limoges, (2006).

[53] Gaudon Alexandre, thèse de Doctorat, Matériaux composites nano structurés par séparation de phases dans le système silice-zircone, Limoges, (2005).

[54] J. Livage, Sol-gel synthesis of solids, Encyclopedia of Inorganic Chemistry, R. Bruce King and. John Wiley edition, New York, 3836-3851, (1994).

[55] https://str.llnl.gov/str/May05/Satcher.html, Novel Materials from Sol-gel Chemistry, Lawrence Livermore National Laboratory, 2005.

[56] L. Holland, Vacuum deposition of thin films. First Edition, Published 1956 by Wiley & Sons.

[57] P. S. Patil, " Versatility of chemical spry pyrolysis technique", Material Chemistry and Physics vol. p.59, (1999).

[58] D. A. Neaman, "Semiconductor physics and Devices", Basic principles, Richard D. Irwin Inc, London, (1992).

[59] H. Sato, T. Minami, S. Takata,T. Yamada," Transparent conducting p-type NiO thin films prepared by magnetron sputtering "Thin Solid Films, vol. 236 pp.27-31, (1993).

[60] J. C. Vigine, J. Spitz , J. Electrochem, "Chemical Vapor Deposition at Low Temperatures", Soc, vol. 15, pp. 122, 585, (1975).

[61] S. Pawar, synthesis and characterization of Sm0.5Sr0.5CoO3 films for solid oxide fuel cell application, PhD thesis, Shivaji University Kolhapur, (2011).

[62] Lilia Baghriche, thèse de Doctorat, Elaboration et caractérisation des couches Minces d'oxyde de zinc et sulfure de zinc préparé par spray ultrasonique, Université Frères Mentouri, Algérie (2015).

[63] Ibrahima Soumahoro, thèse de Doctorat, Elaboration et caractérisation des couches Minces de ZnO dopées au molybdène et à l'ytterbium, pour des applications photovoltaïques, Université Mohammed V, Maroc (2012).

[64] P. S. Patil, " Versatility of chemical spry pyrolysis technique", Material Chemistry and Physics vol. p.59, (1999).

[65] G. Slewah, "Study of Electrical and Optical Properties of Thin Film of CdS and CdS: In Prepared by Spray Pyrolysis Technology ", M.Sc. Thesis, College of Sciences, University of Basrah, Iraq (1990).

[66] K. Reichelt, "Nucleation and growth of thin films", J. Vacuum, Vol. 38, No. 12, 1083-1099, (1988).

[67] A. Beggas, "Elaboration and characterization of chalcogenide thin films by chemical bath deposition technique", Doctoral Thesis, Biskra University, Alegria, (2018).

[68] M. Thomson,"The Modification of Thin Film Surface Structure via Low Temperature Atmospheric Pressure CVD Post Process Treatment Material", Doctoral Thesis, Sanford Greater Manchester University, United Kingdom (2013).

[69] J. A. Nielsen and D. McMorrow, "Element of modern X-ray physics", WILY Edition, Second Edition, ISBN: 978-0-470-97394-3, (2011).

[70] V. Saravanakannan and T. Radhakrishnan, "Structural, electrical and optical characterization of CuO thin films prepared by spray pyrolysis technique", International Journal of Chem Tech Research, Vol. 6, No. 1, 306-310,(2014).

[71] A. Rahdar, M. Aliahmadb and Y. Azizi, "NiO Nanoparticles: Synthesis and Characterization", Journal of Nanostructures, Vol. 5,145-151, (2015).

[72] L. Cattin, B. A. Reguig, A. Khelil, M. Morsli, K. Benchouk and J. C. Berne `de, "Properties of NiO thin films deposited by chemical spray pyrolysis using different precursor solutions", Applied Surface Science, Vol. 254, 5814-5821, (2008).

[73] O. Belahssen, M. Ghougali and A. Chala, "Effect of iron doping on physical properties of NiO thin films", Journal of Nano-and Electronic Physics, Vol. 10, No. 2, 1-4 ,(2018).

[74] M. Mekhnache, A. Drici, L. S. Hamideche, H. Benzarouk, A. Amara, L. Cattin, J. C. Bernede and M. Guerioune, "Properties of ZnO thin films deposited on (glass, ITO and ZnO: Al) substrates", Super lattices and Microstructures, Vol. 49, No. 5,510-518, (2011).

[75] M. V. Kumar, S. Muthulakshmi, A. A. Paulfrit, J. Pandiarajan, N. Jeyakumaran and N. Prithivikumaran, "Structural and optical behavior of thermally evaporated p-Type Nickel Oxide thin film for Solar Cell Applications", International Journal of Chem Tech Research, Vol. 6, No. 13, 5174-5177 ,(2014).

[76] M. Karunakaran, S. Maheswari, K.Kasirajan and S. Dineshraj, "Physical properties of Nano-crystalline Tin Oxide thin film by chemical spray pyrolysis method", International Journal for Research in Applied Science & Engineering Technology, Vol. 4, No. 7, 691-695,(2016).

[77] A. F. Saleh, "Structural and morphological studies of NiO thin films prepared by Rapid thermal oxidation method", International Journal of Application or Innovation in Engineering & Management, Vol. 2, No. 1,16-21 ,(2013).

[78] Y. Z. Dawood, M. H. Hassoni and M. S. Mohamad, " Effect of solution concentration on some optical properties of indium oxide doped with SnO2 thin films prepared by chemical spray pyrolysis technique", International Journal of Pure and Applied Physics, Vol. 2, No. 1, 1-7 ,(2014).

[79] S. Ilican, M. caglar, Y. caglar, "Determination of the thickness and optical constants of transparent indium-doped ZnO thin films by the envelope method", Materials Science-Poland, Vol. 25, No. 3,709-718,(2019).

[80] M. caglar, Y. caglar, S. Ilican, "The determination of the thickness and optical constants of the ZnO crystalline thin film by using envelope method", Optoelectronics and Advanced Materials, Vol. 8, No. 4, 1410-1413, (2006).

[81] L. Reimer, "Scanning Electron Microscopy: Physics of image formation and microanalysis", springer-verlag, Second Edition, ISBN 3-540-63976-4, (1998).

[82] E. Suzuki, "High-resolution scanning electron microscopy of immune gold-labeled cells by the use of thin plasma coating of osmium". Journal of Microscopy, Vol. 208, No. 3,153-157, (2002).

[83] A. R. Xarouco de Barros, "Development of p-type oxide semiconductors based on tin oxide and its alloys: application to thin film transistors", Master Thesis, Lisbon University, Portugal, (2014).

[84] S. Benhamida, "Caractérisation Des Couches Minces D'oxyde De Nickel (NiO) Elaboré Par Spray Pyrolyse", Doctoral Thesis, Biskra University, Algérie, (2018).

[85] P. Miles, "High transparency infrared materials - A technology update", Optical Engineering, Vol. 15, 451-459, (1976).

[86] A. V. Rajgure, "Synthesis and Characterization of nano-crystalline ZnO gas sensor", Doctoral Thesis, Solapur University, India, (2014).

[87] B. A. Ezekoye and C.E. Okeke, "Optical properties in PbHgS ternary thin films deposited by solution growth method", The Pacific Journal of Science and Technology, Vol. 7. No. 2, 108-113, (2006).

[88] A. D. A. Buba and J. S. A. Adelabu, "Optical and Electrical Properties of Chemically Deposited ZnO Thin Films", The Pacific Journal of Science and Technology, Vol. 11, No. 2, 429-434, (2014).

[89] S. S. Roy and J. Podder, "Synthesis and optical characterization of pure and Cu doped SnO2 thin films deposited by spray pyrolysis", Journal of Optoelectronics and Advanced Materials, Vol. 12, No. 7, 1479 -1484, (2010).

[90] F. N. Al.Shammary, "Optical characteristics of NiO thin film on glass formed by Chemical spray pyrolysis", Journal of Kufa – Physics, Vol. 2, No. 1, 22-27, (2010).

[91] S. Sriram and A. Thayumanavan, "Structural, optical and electrical properties of NiO thin films prepared by low cost spray pyrolysis technique", International Journal of Materials Science and Engineering, Vol. 1, No. 2, 118-121, (2013).

[92] N. N. Jandow, "Effects of Cu-doping on optical properties of NiO", International Letters of Chemistry, Physics and Astronomy, Vol. 48, 155-162, (2015).

[93] K.Boubaker, "A physical explanation to the controversial Urbach tailing universality, The European Physical Journal Plus", Vol. 126, No. 10, 1-4, (2011).

[94] F. N. C. Anyaegbunam and C. Augustine, " A study of optical band gap and associated Urbach energy tail of chemically deposited metal oxides binary thin film", Digest Journal of Nanomaterial's and Biostructures, Vol. 13, No. 3, 847-856, (2018).

[95] K. Anandan and V. Rajendran, "Effect of Fe Doping in NiO Semiconductor Nanoparticles and Studies on Their Structural, Magnetic and Optical Properties: Synthesized Via the Precipitation Process", International Journal of Advanced Trends in Engineering and Technology, Vol. 2, No. 2, 1-5, (2017) .

[96] S. Bebramache, Y. Aoun, S. Lakel, B. Benhaoua and C. Torchi, "The calculate of optical gap energy and Urbach energy of Ni1-xCoxO thin films", Journal of Sãdhanã, Vol. 44, N. 26 , 1-6, (2019).

[97] R. K. Al-Hakim, Adel Khudair Hussain, The Foundations of Electronic Engineering, Ministry of Higher Education Press, Baghdad (1980).

[98] S A. Vanalakar, chemical synthesis of cds, ZnO and CdS sensitized ZnO thin films and their characterization for photo-electrochemical solar cells, PhD thesis, Shivaji University, Kolhapur, (2010).

[99] Shewale, Prashant Shivaji. "Synthesis of ZnO Thin Films by Advanced Spray Pyrolysis Technique and their Use in Gas Sensor." (2017).